

UNCLASSIFIED

AD NUMBER
AD478182
NEW LIMITATION CHANGE
TO Approved for public release, distribution unlimited
FROM Distribution authorized to U.S. Gov't. agencies and their contractors; Administrative/Operational Use; DEC 1965. Other requests shall be referred to Air Force Materials Laboratory, Attn: Metals and Ceramics Division, Wright-Patterson AFB, OH 45433.
AUTHORITY
AFSC/IST [WPAFB, OH] ltr, 21 Mar 1989

THIS PAGE IS UNCLASSIFIED

AD 478182

AFML-TR-65-2
Part I, Volume V

TERNARY PHASE EQUILIBRIA IN TRANSITION METAL-
BORON-CARBON-SILICON SYSTEMS

Part I. Related Binary Systems

Volume V. Ta-C System. Partial Investigation in the
Systems Nb-C and V-C

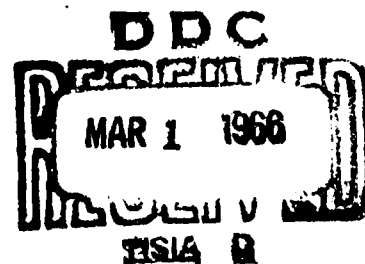
E. Rudy
D. P. Harmon

Aerojet-General Corporation

TECHNICAL REPORT NO. AFML-TR-65-2, Part I, Volume V
December 1965

This document is subject to special export controls and each transmittal to foreign governments or foreign nationals may be made only with prior approval of Metals and Ceramics Division, Air Force Materials Laboratory, Wright-Patterson AFB, Ohio.

Air Force Materials Laboratory
Research and Technology Division
Air Force Systems Command
Wright-Patterson Air Force Base, Ohio



30290

DDG FILE COPY

NOTICES

When Government drawings, specifications, or other data are used for any purpose other than in connection with a definitely related Government procurement operation, the United States Government thereby incurs no responsibility nor any obligation whatsoever; and the fact that the Government may have formulated, furnished, or in any way supplied the said drawings, specifications, or other data, is not to be regarded by implication or otherwise as in any manner licensing the holder or any other person or corporation, or conveying any rights or permission to manufacture, use, or sell any patented invention that may in any way be related thereto.

2		

Copies of this report should not be returned to the Research and Technology Division unless return is required by security considerations, contractual obligations, or notice on a specific document.

18 AFML TR-65-2-Pt-1-Vol-5
Part I, Volume V

19
6 TERNARY PHASE EQUILIBRIA IN TRANSITION METAL-
BORON-CARBON-SILICON SYSTEMS,

Part I. Related Binary Systems.

Volume V. Ta-C System. Partial Investigation in the
Systems Nb-C and V-C.

9 Technical rept.,

10 E. Rudy
D. P. Harmon.

This document is subject to special export controls and each transmittal to foreign governments or foreign nationals may be made only with prior approval of Metals and Ceramics Division, Air Force Materials Laboratory, Wright-Patterson AFB, Ohio.

11 Dec 65, 12 1967.

15 AF 33(615)-1249

16 AF-7350

17 735001

FOREWORD

The research described in this report was carried out at the Materials Research Laboratory, Aerojet-General Corporation, Sacramento, California, under USAF Contract No. AF 33(615)-1249. The contract was initiated under project No. 7350, Task No. 735001, and was administered under the direction of the Air Force Materials Laboratory, Research and Technology Division, with Captain R. A. Peterson acting as Project Engineer, and Dr. E. Rudy, Aerojet-General Corporation, as Principal Investigator. Dr. Hans Nowotny, University of Vienna, served as consultant to the program.

The project, which includes the experimental and theoretical investigation of related binary and ternary systems in the system classes $\text{Me}_1\text{-Me}_2\text{-C}$, Me-B-C , $\text{Me}_1\text{-Me}_2\text{-B}$, Me-Si-B , and Me-Si-C , was initiated on 1 January 1964. The work on related binary systems Me-C and Me-B was initiated in November 1964 as a subtask to the investigation of the ternaries.

The authors wish to acknowledge the assistance of C. E. Brukl and St. Windisch in the work on this system. Contributions were also made by T. Eckert (DTA-runs), J. Pomodoro and R. Taylor (sample preparation), J. Hoffman (metallographic preparation) and R. Cobb (X-ray exposures). The chemical analytical work was carried out under the supervision of W.E. Trahan, Quality Control Division, Solid Rocket Operation.

The help of Mr. R. Cristoni in preparing the numerous drawings, and of Mrs. J. Weidner, who typed the report, is gratefully acknowledged.

The manuscript of this report was released by the authors December 1965 for publication as an RTD Technical Report.

Other reports issued under USAF - Contract AF 33(615)-1249 have included:

Part I. Related Binaries

- Volume I. Mo-C-System
- Volume II. Ti-C and Zr-C Systems
- Volume III. Mo-B and W-B Systems
- Volume IV. Hf-C System

Part II. Ternary Systems

- Volume I. Ta-Hf-C System
- Volume II. Ti-Ta-C System
- Volume III. Zr-Ta-C System


Part III. Special Experimental Techniques

- Volume I. High Temperature Differential Thermal Analysis

Part IV. Thermochemical Calculation

Volume I. Thermodynamic Properties of Group IV,
V, and VI Binary Transition Metal
Carbides

This technical report has been reviewed and is approved.



W. G. RAMKE

Chief, Ceramics and Graphite Branch
Materials and Ceramics Division
Air Force Materials Laboratory

ABSTRACT

The alloy system tantalum-carbon was investigated by means of X-ray, DTA, and melting point techniques on heat-treated and chemically analyzed alloys; a complete phase diagram was established.

Analogously to the findings in the Ta-C systems, a previously unknown phase reaction of the Nb_2C phase was found to occur at high temperatures. The melting temperatures of the monocarbide phase and the NbC-C eutectic reaction isotherm were redetermined.

The α - β - Me_2C -phase reaction could not be found in the vanadium-carbon system.

The results are discussed, and compared with previously reported system data.

TABLE OF CONTENTS

	PAGE
I. INTRODUCTION AND SUMMARY	1
A. Introduction	1
B. Summary.	1
1. Tantalum-Carbon	1
2. Niobium-Carbon.	5
3. Vanadium-Carbon.	6
II. LITERATURE REVIEW.	6
III. EXPERIMENTAL PROGRAM.	11
A. Starting Materials	11
B. Experimental Procedures	13
1. Sample Preparation and Heat-Treatment . . .	13
2. Differential Thermal Analysis.	14
3. Melting Points.	14
4. X-Ray Analysis	17
5. Metallography	17
6. Chemical Analysis.	20
C. Results	21
1. Tantalum-Carbon.	21
2. Niobium-Carbon and Vanadium-Carbon. . . .	64
IV. DISCUSSION	70
A. The α - β -Ta ₂ C Phase Reaction	70
B. Phases and Phase Equilibria	74
References	76

ILLUSTRATIONS

FIGURE		PAGE
1	Phase Diagram Tantalum-Carbon	2
2	Nb-C: Melting Temperatures of the Monocarbide Phase and the Carbon-Rich Eutectic	5
3	Phase Diagram Tantalum-Carbon	7
4	Lattice Parameter of TaC_{1-x}	10
5	Post-Experiment Section of a Ta-20 At% C DTA-Sample	15
6	Post-Experiment Appearance of a Pirani Melting Point Specimen	18
7	Specimen of Figure 6, Sectioned	19
8	Differential Cooling Curves of a Tantalum-Carbon Alloy with 8 Atomic % Carbon.	22
9	Ta-C (4 At% C), Cooled at Approximately $40^{\circ}C \cdot sec^{-1}$ From $2900^{\circ}C$	23
10	Ta-C (7 At% C), Pre-equilibrated at $2800^{\circ}C$, Cooled with $4^{\circ}C \cdot sec^{-1}$ to $2500^{\circ}C$, and Quenched ($100^{\circ}C \cdot sec^{-1}$)	24
11	Ta-C (8 At% C), Pre-equilibrated at $2840^{\circ}C$, Cooled with $4^{\circ}C \cdot sec^{-1}$ to $2200^{\circ}C$, and Quenched ($100^{\circ}C \cdot sec^{-1}$)	25
12	Ta-C (6 At% C), Cooled at Approximately $1^{\circ}C \cdot sec^{-1}$ From $2800^{\circ}C$,	27
13	Ta-C (8 At% C), Cooled at Approximately $4^{\circ}C \cdot sec^{-1}$ From $2800^{\circ}C$,	27
14	Ta-C (8 At% C), Quenched from $2870^{\circ}C$,	28
15	Ta-C (12 At% C), Quenched from $2850^{\circ}C$,	28
16	Ta-C (17 At% C), Cooled at $16^{\circ}C \cdot sec^{-1}$ from $3100^{\circ}C$	29
17	Ta-C (25.5 At% C), Quenched From $2860^{\circ}C$	29

ILLUSTRATIONS (Cont.)

FIGURE		PAGE
18	Ta-C (26 At% C), Quenched from 2870°C.	30
19	Melting Temperatures of Tantalum-Carbon Alloys.	31
20	DTA-Thermogram of Tantalum-Carbon Alloy With 21 Atomic % Carbon.	32
21	Differential Heating and Cooling Curve of a Tantalum-Carbon Alloy with 30 Atomic % Carbon.	33
22	Differential Heating and Cooling Curve of a Tantalum-Carbon Alloy with 32 Atomic % Carbon.	34
23	Differential Heating and Cooling Curve of a Tantalum-Carbon Alloy with 33 Atomic % Carbon.	35
24	Differential Cooling Curve of a Tantalum-Carbon Alloy with 33 Atomic % Carbon.	36
25	Differential Heating and Cooling Curve of a Tantalum-Carbon Alloy with 36 Atomic % Carbon.	36
26	Differential Cooling Curves of Tantalum-Carbon Alloys with 37 and 38 Atomic % Carbon.	37
27	α - β -Ta ₂ C Phase Reaction as a Function of the Carbon Concentration.	38
28	α - β -Ta ₂ C Reaction Under Rapid Cooling Conditions: Differential Cooling Curves of Alloys in the Range from 30 to 42 Atomic % Carbon.	39
29	Tantalum-Carbon: Position and Qualitative X-Ray Evaluation of the Alloys for the Investigation of the Solid State Portion of the System.	41
30	Ta-C (30 At% C) Rapidly Cooled ($40^{\circ}\text{C}\cdot\text{sec}^{-1}$) from 3380°C.	42
31	Ta-C (29 At% C), Quenched from 3050°C.	44
32 (a & b)	Tantalum-Carbon Diffusion Couple, 1 hr at 2850°C.	46
33 (a & b)	Ta-C Diffusion Couple, 15 min at 3000°C (Cooled at $14^{\circ}\text{C}\cdot\text{sec}^{-1}$).	47

ILLUSTRATIONS (Cont.)

FIGURE		PAGE
34	Ta-C: Diffusion Couple Shown in Figure 32; Enlargement of Ta ₂ C-Liquid Interface.	48
35	Ta ₂ C-C Diffusion Couple, 15 min at 3200°C.	49
36	Ta-C: Diffusion Couple. Substructure Developed in Ta ₂ C after Rapid Quenching from 2800°C.	50
37	Ta-C Diffusion Couple. Sample from Figure 36, Ta ₂ C Layer, Under Higher Magnification.	50
38	Ta-C (~ 34 At% C), Quenched from 3100°C, and Heat-Treated for 24 hrs at 1750°C,	51
39	Ta-C (35 At% C), Quenched from 3250°C, and Heat-Treated for 225 hrs at 1600°C,	52
40	Ta-C (33.3 At% C), Quenched from 3000°C and Heat-Treated for 225 hrs at 1600°C.	52
41	Ta-C (38 At% C), Quenched from 3300°C.	53
42	Ta-C (40 At% C), Cooled at 100°C·sec ⁻¹ from 3500°C,	56
43	Ta-C (42 At% C), Cooled at 100°C·sec ⁻¹ from 3700°C,	56
44	Ta-C (37 At% C), Cooled at 5°C·sec ⁻¹ from 3300°C.	57
45	Ta-C (39 At% C), Cooled at 5°C·sec ⁻¹ from 3300°C.	57
46	Ta-C (37 At% C), Cooled at 5°C·sec ⁻¹ from 3300°C and Heat-Treated for 24 hrs at 1700°C.	59
47	Ta-C (39 At% C), Quenched from 3500°C and Annealed for 24 hrs at 1700°C,	59
48	Ta-C (49.3 At% C), Quenched from 3450°C.	60
49	Ta-C (50.2 At% C), Quenched from 3500°C.	60
50	Ta-C (51.5 At% C), Quenched from 3480°C.	61
51	DTA-Thermogram of a Ta-C Alloy with 70 Atomic % Carbon, Showing Eutectic Melting (Heating and Solidification (Cooling) at ~ 3440°C.	62

ILLUSTRATIONS (Cont.)

FIGURE		PAGE
52	Ta-C (55 At% C), Quenched from 3480°C.	63
53	Ta-C (61 At% C), Quenched from 3450°C.	63
54	DTA-Thermogram of a Niobium Carbon Alloy with 25 Atomic % Carbon.	66
55	Differential Heating and Cooling Curve of a Niobium-Carbon Alloy with 30 Atomic % Carbon.	67
56	Differential Heating and Cooling Curve of a Niobium-Carbon Alloy with 32 Atomic % Carbon.	68
57	Differential Heating and Cooling Curves of a Niobium-Carbon Alloy with 34 Atomic % Carbon.	69

TABLE	TABLES	PAGE
1	Isothermal Reactions in the System Tantalum-Carbon	3
2	Terminal Solid Solubility of Carbon in Tantalum	8
3	Reported Melting Temperatures for Tantalum Monocarbide	11
4	Observed Melting Point of Tantalum as a Function of the Total Impurity Content	21
5	Melting Temperatures of Tantalum-Carbon Alloys	26
6	Lattice Parameters of Ta_2C	40
7	Compositions of the Liquidus in Equilibrium with Ta_2C	51

I. INTRODUCTION AND SUMMARY

A. INTRODUCTION

In continuation of our efforts on the elucidation of the high temperature phase relationships in binary and ternary systems of refractory transition metals with carbon, boron, and silicon, this time, the clarification of the phase-relationships in the group V metal-carbon systems was the aim of our investigations.

Comprehensive investigations were performed only on the tantalum-carbon system, since the gross-features of the phase-relationships in the systems of niobium and vanadium with carbon were available from recent works by E.K. Storms, et.al.^(1,2) Special attention in the investigations was devoted to the study of the thermal behavior of the Me_2C -phases, with the specific intent to search for phenomena related to the temperature-activated disordering of the carbon sublattices in these compounds⁽³⁻⁶⁾.

B. SUMMARY

1. Tantalum-Carbon

Based on X-ray and metallographic investigations on heat-treated and quenched alloy material, as well as on the results obtained from differential-thermal analysis and melting point determinations, a phase diagram for the system tantalum-carbon was established (Figure 1, Table 1).

The results are summarized as follows:

a. α -Tantalum

Pure tantalum melts at $3014 \pm 10^\circ\text{C}$. The metal solid solution extends to 7.5 At% carbon at 2843°C , the temperature of the Ta-Ta₂C eutectic.

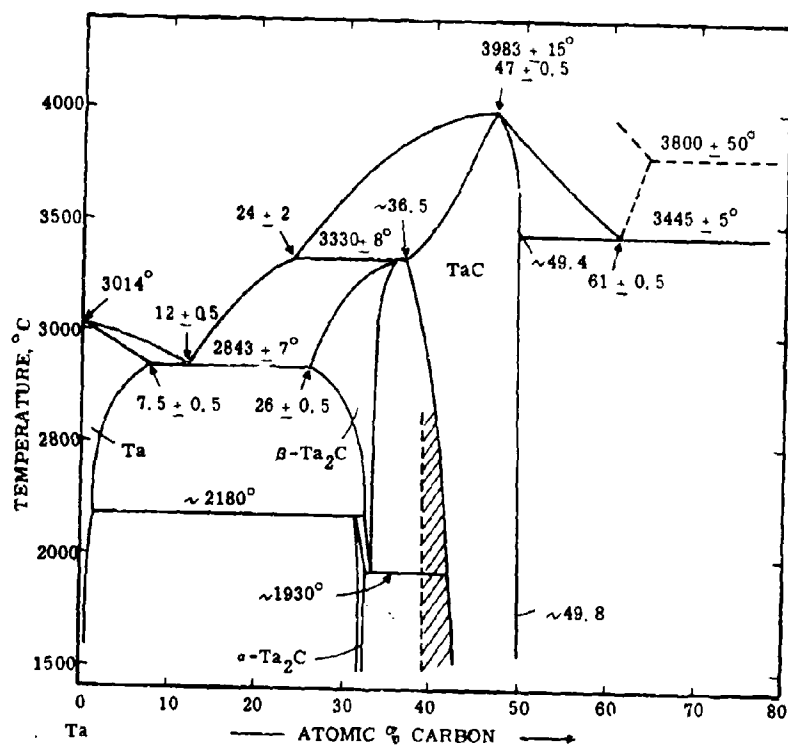


Figure 1. Phase Diagram Tantalum-Carbon

Shaded Area: Preferred Precipitation of (Metastable)γ.

b. α -Ta₂C

α -Ta₂C, with a hexagonal close-packed arrangement of metal atoms, extends at 1700°C from approximately 31.5 to 33 At% C ($a = 3.100$ to 3.102 \AA ; $c = 4.931$ to 4.940 \AA). The phase decomposes in a peritectoid reaction at 2180°C into β -Ta₂C and tantalum.

c. β -Ta₂C

β -Ta₂C, with a hexagonal close-packed arrangement of metal atoms, is formed in a peritectic reaction at 3330°C according to $P (24 \text{ At\% C}) + B1 (36.5 \text{ At\% C}) \rightarrow \beta\text{-Ta}_2\text{C} (\sim 35.5 \text{ At\% C})$.

Table 1. Isothermal Reactions in the System Tantalum-Carbon

Temperature, °C	Reaction	Compositions of the Equilibrium Phases, At% C	Type of Reaction
3983 ± 15°	L ± 8	47 + 0.5 47 + 0.5 -	Congruent Transformation
3445 ± 5°	L ± δ + C	61.0 + 0.5 49.5 + 0.2 ~100	Eutectic Reaction
3330 ± 8°	L + δ ± β'	24 ± 2 36.6 ± 1 35.5 ± 1	Peritectic Reaction
2843 ± 7°	L ± α + β'	12 ± 0.5 7.5 ± 0.5 26 ± 0.5	Eutectic Reaction
2180 ± 20°	α + β' ± β	~ 0.5 33.5 ± 0.5 31.0 ± 1	Peritectoid Reaction
1930 ± 30	β' ± β + ζ	34.0 ± 1 32.0 ± 1 39 ± 1	Peritectoid Reaction

Legend:

L - Liquid

α - Tantalum-phase

β, β' - Low and High Temperature Modifications of Ta₂C

ζ - Bauer's zeta phase at ~39 At% C

δ - Cubic monocarbide phase

The phase, which extends at the Ta-Ta₂C eutectic temperature (2843°C) from 26 to ~34 At% carbon, decomposes in a rapid eutectoid reaction into α-Ta₂C and monocarbide phase. The eutectoid point is located at 33.5 At% C and 1930 ± 30°C.

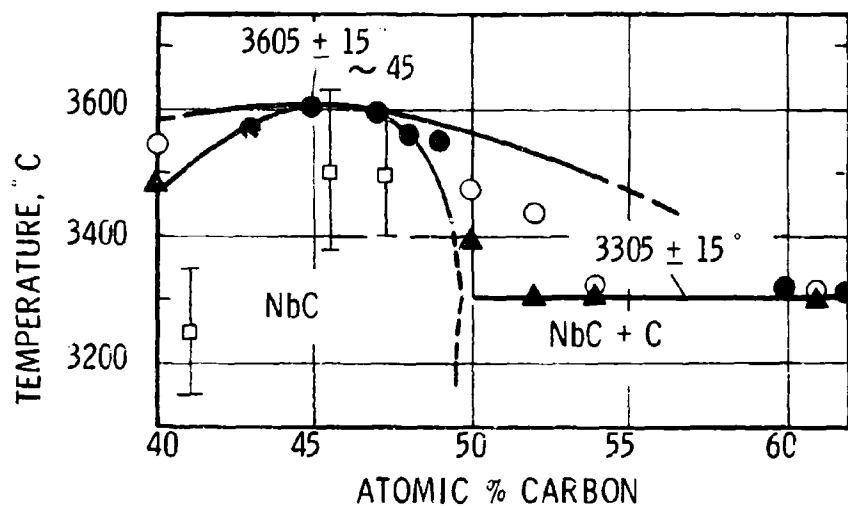
The α-β-Ta₂C phase reaction can be interpreted as being the result of an order-disorder transformation of the carbon sublattice, proceeding within a structurally unchanged metal host lattice.

d. ζ-TaC_{1-x} (Metastable Pseudophase)

ζ-TaC_{1-x} (stable only in the form of thin epitaxial platelets on TaC_{1-x}), is formed by localized precipitation from substoichiometric tantalum monocarbide. In bulk form it is unstable with regard to a mechanical mixture of sub- and monocarbide. The structure of the ζ-precipitate is unknown, but the diffraction patterns indicate close similarity to the B1-type of monocarbide as well as the hcp-type lattice of the subcarbide, (transition type).

e. δ-TaC

δ-TaC has a sodium chloride, B1 type of structure with $a = 4.456 \text{ \AA}$ (49.8 At% C), and melts congruently at a composition of 47 At% C and a temperature of 3983°C. The homogeneous range of the phase extends from 36.6 to ~49.7 At% C at 3330°C, from ~40 to 49.8 At% C at 2400°C, and from 42.5 At% C ($a = 4.412 \text{ \AA}$) to 49.8 At% C ($a = 4.456 \text{ \AA}$) at 1700°C. The phase forms a eutectic with graphite (61 At% C, 3445°C).



- ▲ Incipient Melting
- Sample Collapsed
- Sharp Melting ($T_{inc} = T_{coll.}$)
- E. K. Storms and N. H. Krikorian, 1960

Figure 2. Nb-C: Melting Temperatures of the Monocarbide Phase and the Carbon-Rich Eutectic

2. Niobium-Carbon

A partial investigation of the system included the following results:

a. Nb_2C

Nb_2C with a close-packed arrangement of metal atoms undergoes a rapid phase transition at temperatures of approximately $2460^\circ C$. The transition temperature is practically concentration-independent. Based on indirect evidence, the transformation is to be attributed to a disordering reaction of the carbon sublattice, i.e. the phase reaction does not involve a structural change of the metal host lattice.

b. Niobium Monocarbide (Figure 2)

The face-centered (B1-type) monocarbide melts congruently at $3605 \pm 15^\circ\text{C}$ at a composition of $\sim 45 \text{ At\% C}$. A eutectic reaction occurs between NbC and graphite at $3305 \pm 15^\circ\text{C}$; the eutectic composition is located at approximately 60 atomic % carbon.

3. Vanadium-Carbon

In DTA-studies covering the temperature range from 800 to 2300°C no thermal arrest were detected which could be associated with an order-disorder type reaction of the carbon sublattice analogous to the transformations of the other Me_2C -phases of the group V and group VI transition metals. Increasing substitution of the metal atoms in Mo_2C , W_2C , and ' Cr_2C ' by vanadium show a decrease of the order-disorder transformation temperatures of these compounds, indicating that a possible order-disorder reaction in V_2C would have to occur at temperatures below 800°C .

II. LITERATURE REVIEW

The first complete investigation of the tantalum-carbon system was performed by E. H. Ellinger⁽⁷⁾ in 1943. Although the system has been reinvestigated numerous times^(8, 9, 10, 11, 12), the diagram remains basically as initially presented (Figure 3)⁽⁴⁰⁾.

The carbon solubility in tantalum has generally been reported to be low^(7, 8, 13) ($< 0.3 \text{ At\% C}$); however recent work by E. Fromm and U. Roy⁽¹⁴⁾ indicates a rapid increase of the solubility towards higher temperatures (Table 2).

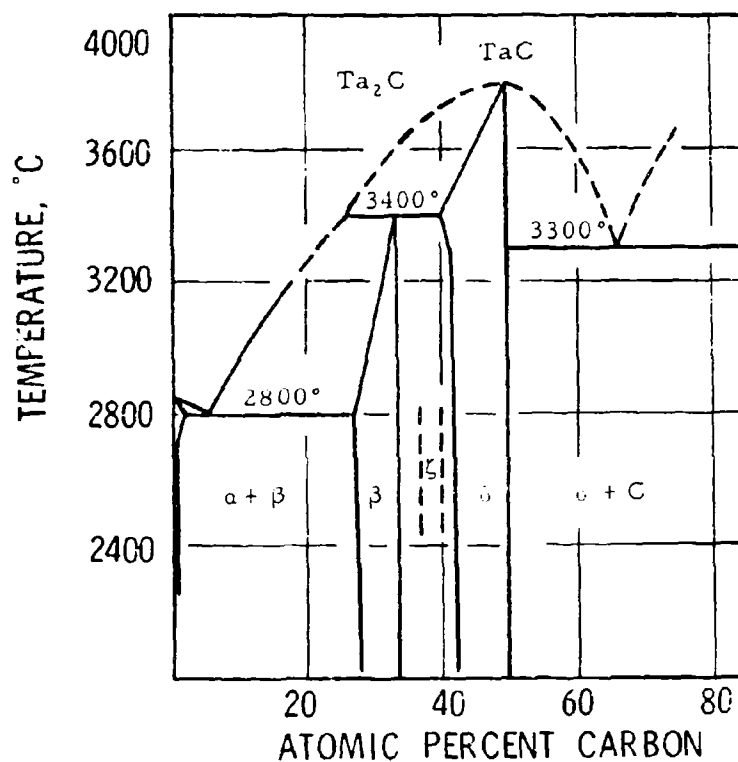


Figure 3. Phase Diagram Tantalum-Carbon

(F.H. Ellinger, 1943, Supplemented by R. Kieffer and F. Benesovsky, 1963)

Eutectic melting between the metal and Ta_2C phases occurs in the vicinity of 2800°C. Recent data for the eutectic point are: 2800°C and 8.1 At% C⁽⁷⁾; 11 At% C⁽⁸⁾; 2902 ± 30°C⁽⁹⁾, and 2825° and 12.5 At% C⁽¹²⁾.

Two stable intermetallic phases, Ta_2C and TaC , are known, and the presence of a third phase (ζ) of low stability has been observed by

Table 2. Terminal Solid Solubility of Carbon in Tantalum
(E. Fromm and U. Roy, 1965).

Temperature °C	Solid Solubility of C At%
1600	0.6
2000	2.3
2400	4.5
2800	~7.5

R. Lesser and G. Brauer⁽¹⁵⁾. The exact location and structure of the latter phase has not been clarified.

The Ta_2C phase crystallizes hexagonally, with the metal atoms in a close-packed arrangement^(7, 16) ($a = 3.106 \text{ \AA}$ and $c = 4.949 \text{ \AA}$)⁽¹⁵⁾. According to F. H. Ellinger⁽⁷⁾ the phase forms in a peritectic reaction from liquid and monocarbide at 3400°C ; subsequent investigations yielded for the peritectic temperature 3500°C ⁽⁹⁾, and 3240°C ⁽¹²⁾. The Ta_2C phase is found to exhibit a range of homogeneity; various investigations have found this range to be between $TaC_{0.47}$ to $TaC_{0.50}$ ⁽⁷⁾, $TaC_{0.38}$ to $TaC_{0.50}$ ⁽¹⁷⁾, $TaC_{0.41}$ to $TaC_{0.50}$ ⁽¹⁵⁾, $TaC_{0.43}$ to $TaC_{0.50}$ (2200°C)⁽¹⁸⁾, and $TaC_{0.36}$ to $TaC_{0.50}$ (2825°C)⁽¹²⁾. I. G. McMullin and J. T. Norton⁽¹⁹⁾ find the upper boundary at $TaC_{0.46}$, whereas Santoro and Probst⁽¹¹⁾ have presented evidence for the upper boundary to extend to hyperstoichiometric compositions. The lattice parameters at the low carbon boundary, taken from Lesser and Brauer⁽¹⁵⁾, are $a = 3.101 \text{ \AA}$, and $c = 4.933 \text{ \AA}$ ($\sim 2000^\circ\text{C}$).

The occurrence of two modifications of Ta_2C was reported by Burgers and Basart⁽¹⁶⁾, but subsequent works have not confirmed this observation^(7, 12, 20).

In the discussion of Ellinger's⁽⁷⁾ paper, F.N. Rhines suggests that the lamellar structure characteristic of subcarbide with less than ~31.5 atomic % carbon might be a result of a eutectoid decomposition. The original interpretation by (7), that the structure is a result of tantalum precipitation from the subcarbide has been shown to be correct^(11,12).

The extensive interest in the Ta-C phase diagram is due primarily to the very high melting monocarbide phase. E. Friederich and L. Sittig⁽²¹⁾ first reported the melting point to be about 3825°C, a value, which was shortly afterwards confirmed by Agte and H. Alterthum⁽²²⁾ ($3875 \pm 150^\circ\text{C}$). Table 3 gives a compilation of more recent determinations of the TaC melting point; in many of these investigations excessive carbon losses or reaction with the container material were encountered, thus shedding some doubt on the measurements.

The monocarbide phase crystallizes in a body-centered cubic structure (NaCl type)^(25,26), and forms an extended range of carbon defect solid solutions. The homogeneity limits of the monocarbide have been the object of numerous investigations^(12,15,17,18,27,28,29,30); values found by Lesser and Brauer⁽¹⁵⁾ (Figure 4) have been more recently confirmed^(12,18,29,30).

P. T. B. Shaffer⁽³⁾ has cited indirect evidence for a reversible high-temperature transformation in tantalum-monocarbide. However, heat content measurements by L. S. Levenson⁽³²⁾, did not indicate any anomalous behavior.

A eutectic is formed between the monocarbide and graphite. Ellinger⁽⁷⁾ first determined the eutectic point at ~3300°C

and 62.6 atomic % carbon; other determinations are: $3710 \pm 50^\circ\text{C}$ and 56.7 At% C⁽⁹⁾, $3310 \pm 50^\circ\text{C}$ and ~80 At% C⁽³³⁾ and 3375°C and 61.2 At% C⁽¹²⁾.

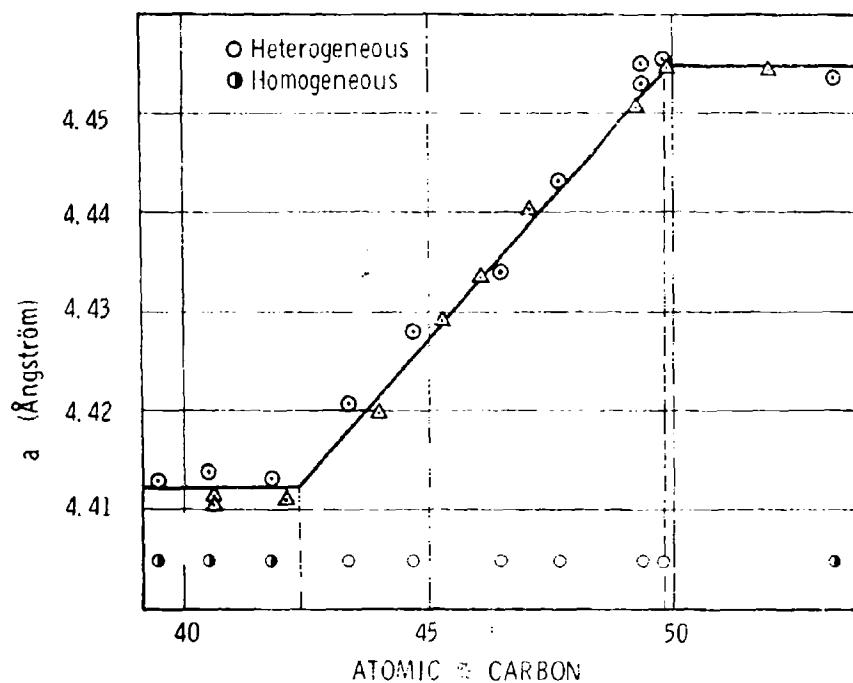


Figure 4. Lattice Parameter of TaC_{1-x}

⊙ R. Lesser and G. Brauer

△ E. Rudy, et al., 1962

Table 3. Reported Melting Temperatures for Tantalum Monocarbide

Investigator	Ref.	Melting Temperatures, °C
E. Friederich & G. Sittig, 1925	21	3825°
G. Agte & H. Alterthum, 1930	22	3875 ± 150°
G.A. Geach & F.O. Jones, 1957	23	3540°
L.D. Brownlee, 1958	24	3780°
M.R. Nadler & C.P. Kempter, 1960	9	> 3550°
C. F. Zalabak, 1961	10	3740°
M. G. Bowman, 1964	20	4000 - 4200°C

III. EXPERIMENTAL PROGRAM

A. STARTING MATERIALS

The powdered elements as well as tantalum monocarbide served as the starting material for the preparation of the experimental alloy material.

Tantalum (99.9 % pure) was purchased in powder from Wah Chang Corporation, Albany, Oregon. Main impurity constituents* were as follows (contents in ppm): C-140, Nb-100, O-280, sum of other impurities - <300. A lattice parameter of $a = 3.30, \text{\AA}$ was obtained from a powder-diffraction pattern with Cu-K_α radiation. This value compares

*The chemical analysis of the starting material was performed under the supervision of Mr. W. E. Trahan, Quality Control Division, Aerojet-General Corporation.

favorably with lattice spacings of $a = 3.302 - 3.303 \text{ \AA}$, given in Pearson⁽³⁴⁾.

The spectrographic grade graphite powder (Union Carbide Corporation, Carbon Products Division) had the following analysis: Sum of metallic impurities (Al + Cu + Mg + Si + Fe) - <9 ppm, ash-<500 ppm, volatile matter-100 ppm. No second phase impurities were detected in the powder patterns, and lattice parameters of $a = 2.463 \text{ \AA}$; $c = 6.72 \text{ \AA}$ (literature values $a = 2.461 \text{ \AA}$; $c = 6.708 \text{ \AA}$ ⁽³⁴⁾) were derived from an exposure with Cu-K radiation.

Tantalum monocarbide was purchased from Wah Chang Corporation, Albany, Oregon. It had a particle size of $10 \pm 1.5 \mu$, and was acid-leached and high vacuum-degassed (2 hrs at 4×10^{-6} Torr and 2200°C), in order to minimize the concentration of low melting contaminants. The lattice parameter of the purified material was $a = 4.455_0 \pm 0.003 \text{ \AA}$. The product had a total carbon content of 6.15% Wt% from which 0.04 Wt% were present in free form. Oxygen, nitrogen, and hydrogen were determined by the gas-fusion technique, using a platinum bath, whereas small impurity contents were determined spectrographically. The impurity concentrations obtained were as follows (contents in ppm): Ti-400, Nb-150, Y-200, O-<20, N-<10, H-not detected, Cr-<25, Co-<10, Fe-<70, B + Mg + Mn + Ni + Pb + Si + Sn-<50.

The alloy samples for the studies in the systems vanadium-carbon and niobium-carbon were prepared from the respective metal powders and graphite.

The niobium powder ($a = 3.301 \text{ \AA}$) (Wah Chang Corporation, Albany, Oregon) had the following impurities (contents in ppm^{*}): Al-<20

^{*}The figures in the brackets refer to our control analysis.

C-50 (120), Cr-25, Cu-100 (<60), Fe-<50 (<50), H-30, Hf-30, Mg-<20, Mo-20, N-68 (140), Ni-20, O-460 (655), Si-<10 (<20), Ta-<500 (<100), Ti-<40, W-1150, Zr-250, C-n.d. (130). Vanadium (99.5%) was purchased as -200 mesh powder from Oregon Metallurgical Corporation, Albany, Oregon, and had the following impurities (contents in ppm)*: C-380, H-20, O-1000 (1140), N-290 (400), Fe-300 (100), Mn-n.d. (40), Si-n.d. (<100), Cr-n.d. (100), Al-n.d. (<300), Ca-n.d. (<30). The lattice parameter of this starting material, derived from an exposure with Cu-K_α radiation and using a cover film to filter out the undesirable fluorescent V-K_α radiation, was $a = 3.031 \text{ \AA}$.

B. EXPERIMENTAL PROCEDURES

1. Sample Preparation and Heat-Treatment

The alloys for the investigations were prepared by hot-pressing of the well-blended powder mixtures and subsequent equilibration of the sintered compacts under high vacuum (5×10^{-5} to 5×10^{-6} Torr). A few alloy buttons were also prepared by arc melting precompacted powder mixtures under a high purity helium atmosphere; this method was discarded, however, since considerable segregation of carbide and metal constituents from the melt occurred, and varying carbon-losses prevented an economic planning of the desired sample compositions.

Melting point samples containing excess metal were prepared by cold-pressing corresponding mixtures of tantalum and tantalum monocarbide in steel dies and subsequent sintering of the green compacts

*The figures in the brackets refer to our control analysis.

at temperatures varying between 1800 and 1900°C under a vacuum of better than 10^{-5} Torr.

Rapid quenching of the specific alloy compositions was achieved by dropping the sample after equilibration at the chosen temperatures into a preheated (300°C) tin bath.

2. Differential Thermal Analysis

Details of the apparatus have been given in earlier reports^(5, 35). For the measurements in the group V metal-carbon system, graphite was solely used as container material. The samples were prepared by cold-pressing as well as by hot-pressing of the well-blended powder mixtures, and the runs were made under a high purity helium atmosphere and also under vacuum. After the runs, the samples were sectioned and analyzed.

At temperatures below the carbon-rich eutectic, carbon pickup was very nominal and confined to a thin outer zone of the sample which was in direct contact with the graphite container (Figure 5). No undesirable interference with the measurements was encountered and the results, obtained on duplicate samples, were reproducible within the error limits of the temperature measurements as well as the chemical analysis. Due to the lack of adequate container materials, the DTA-investigations were restricted to temperatures below the TaC + C eutectic reaction isotherm.

3. Melting Points

The melting temperatures of the alloys were determined with the Pirani technique: A small sample bar with a black-body hole (~ 0.6 mm dia x 4 mm deep) is heated resistively to the temperature of

the phase change. The temperature is measured optically with a disappearing filament type micropyrometer. A detailed description of the apparatus as well as the temperature calibration have been given in an earlier report⁽⁵⁾.



Figure 5. Post Experimental Section of a Ta-20 At% C X3
DTA Sample

Treatment: Five Cycles Between 1000° to 2900°C.

Alloys from the concentration range 0 to 30 At% C were melted under helium at a pressure of 1.5 atmospheres. To diminish the diffusion rate of carbon vapor, and consequently the carbon losses from the sample, the furnace chamber was pressurized to 2 1/2 to 4 1/2 atmospheres for single phased monocarbide alloys. Molten as well as unmolten zones of a large portion of the experimental alloy material was analyzed after the runs. With the exception of excess carbon containing alloys, which were melted under a total inert gas pressure of only 1 1/2 atmospheres and where carbon losses of up to 2 atomic percent were

encountered, the deviations from the nominal compositions was usually less than 0.5 At%. The reproducibility (precision) of the measurements for isothermally melting alloys was in the range from ± 10 to $\pm 15^\circ\text{C}$. The overall temperature uncertainties ($\bar{\sigma}$) can be computed from the standard deviation of the experimentally measured values (σ_m) and the error of the pyrometer calibrations (σ_c) according to

$$\bar{\sigma}^2 = \sigma_m^2 + \sigma_c^2$$

Representative values for σ_c are $\pm 10^\circ\text{C}$ at 2300°C , $\sim \pm 17^\circ\text{C}$ at 3000°C , and $\pm 30^\circ\text{C}$ (estimated) at 4000°C .

As described earlier, excess metal containing melting point samples were prepared by cold pressing, while carbide or excess graphite containing alloys were hot pressed and afterwards ground to the desired dimensions. The samples were clamped between the water-cooled copper electrodes of the furnace, using two tungsten platelets as spacers between the specimen and the electrode faces. After several purge cycles (generally three), power was applied until the sample reached a temperature of 2200 to 2300°C . The specimen was held at this temperature until no further degassing, recognizable in a drop of the chamber vacuum, could be noticed. The chamber was then pressurized with high purity helium and the temperature increased within a time period of 15 to 20 seconds to within $\sim 50^\circ\text{C}$ of the expected solidus temperature. The temperature of the change was then approached at a constant rate of $\sim 5^\circ\text{C}$ per second, until the appearance of melt in the cavity indicated that the solidus temperature had been reached.

Two-phased melting samples show infiltration to the sample surface upon further increase in power and a gradual closure of the black body hole; power rises on isothermally melting specimens do not cause the temperature to increase, but merely increase the size of the melt-vacuole in the interior of the (intentionally) porous sample. This behavior constitutes the specific advantage of the Pirani technique over other methods, as it allows sufficient time for the observer to focus and match the pyrometer filament exactly against the radiation from the black-body cavity. The colder (radiation-cooled) outer sample shell keeps material losses due to diffusion of vapors from the interior to a minimum. Upon further power increases, the melting-front eventually reaches the sample surface or the melt fills up the black body hole (Figures 6 and 7), and finally the specimen collapses.

4. X-ray Analysis

Diffraction patterns were prepared from all experimental alloy material. Since the crystal structures of all phases were known from the literature, only powder diffraction patterns (Cu-K_α) were run.

The exposures were taken in a 57.4 mm camera on a Siemens-Crystalloflex II unit; the Bragg-angles of the diffraction lines were measured on a Siemens-Kirem coincidence scale with micrometer dial (2 mm indicator travel per 0.01 mm translational motion of the measuring slide).

5. Metallography

The specimens, mounted in an electrically conductive combination of copper-coated lucite powder and diallyl-phthalate, were coarse-

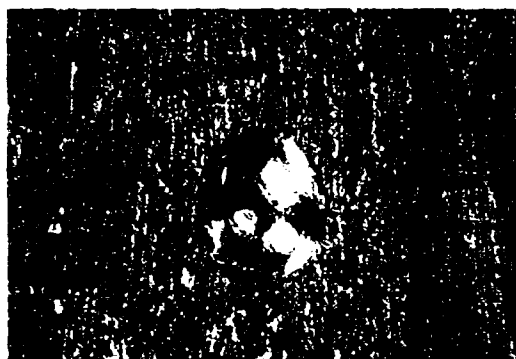


Figure 6. Post-Experimental Appearance of a Pirani ~ X30
Melting Point Specimen

Alloy: Ta-C (47 At% C), With a Measured Melting
Temperature of 3980°C.

Note Black-Body Hole Filled with Melt.

ground on silicon-carbide papers with grit-sizes varying between 120 and 600. Polishing was done on nylon-cloth, using a slurry of 0.05 micrometer alumina powder in a 10% aqueous solution of Murakami's reagent $\{K_3Fe(CN)_6 + KOH\}$. The specimens were then cleaned with a detergent solution, rinsed with ethanol, and dried.

Proper etching of the alloys presented some problems, since the etching behavior varied significantly with the carbon concentration, therefore, a number of different etchant solutions and techniques had to be used in order to develop structural details. Etching of alloys from the subcarbide-monocarbide two-phase region still remains unsatisfactory and needs further improvement.

The structure components in alloys with carbon concentrations from 0-26 atomic percent were differentiated by an anodizing



Figure 7. Specimen in Figure 6, Sectioned.

Note Cavity in the Interior Formed by Infiltration of the Melt Into the Colder Outer Portion of the Porous Specimen.

treatment in a 10% oxalic acid solution. This treatment produced a brownish-red (oxide) tarnish on the tantalum grains, while the carbide grains remained essentially unaffected. Samples with carbon contents between 27 and 44 atomic percent were etched in a solution consisting of 25% HF, 25% HNO₃ and 50% H₂O. Although some etch-pitting could not be avoided, differentiation of the structural elements was acceptable and the grain boundaries clearly distinguishable.

Alloys from the concentration range from 45 to 50 atomic percent carbon were very resistant to etching, and a number of strong acids and stains were used with only moderate success. Acceptable results were achieved using a 20% Murakami's solution, an 8% aqueous solution of potassium permanganate and sodium hydroxide, as well as the above described mixture of HF, HNO₃, and H₂O. For excess graphite-containing alloys, no etching was required, and the samples were examined in the as-polished state.

The exposures were made on a Zeiss Ultraphot II metallograph, using Contrast Process Ortho film by Kodak.

6. Chemical Analysis

The majority of the alloys were analyzed for their carbon content, after the measurements, using the standard combustion technique. Free carbon in excess carbon containing alloys was determined in the well-known manner by determining the amount of carbon-residue left from the dissolution of the powdered alloy in a mixture of hydrofluoric and nitric acid.

Low-concentration impurities in the starting materials were determined spectrographically (section III-A). Oxygen and nitrogen in the alloys was determined by gas-fusion analysis using a platinum-bath. The oxygen contents of processed (heat-treated or melted alloys) were in all cases below 200 ppm.

C. RESULTS

1. Tantalum-Carbon

a. The Tantalum Phase

A melting point of $3014 \pm 10^\circ\text{C}$ was derived from six measurements on samples with total impurity contents (O + N + Fe + Si) of less than 150 ppm. Lower values were measured on less purer starting materials (Table 4).

Table 4. Observed Melting Point of Tantalum as a Function of the Total Impurity Content

Total Impurity Content (Interstitial + Metallic) ppm	Number of Runs	Mean Value, $^\circ\text{C}$	Standard Deviation, $\pm ^\circ\text{C}$
<150	6	3014	10
<300	3	3006	14
~500	2	2985	10
~900	3	2960	15

The solidus temperature of the tantalum phase (Table 5) is gradually lowered by incorporation of carbon atoms into the lattice (2843°C at 7.5 At% C, Figure 1). The solid solubility of carbon in tantalum is strongly temperature-dependent (2843°C : 7.5 At% C; 2500°C : ~2.5 At% C, (Figure 1). The precipitation reaction upon cooling is highly exothermic as evidenced by the DTA-thermograms in Figure 8. This behavior indicates that considerable lattice strain may be involved in the formation of the solution. The

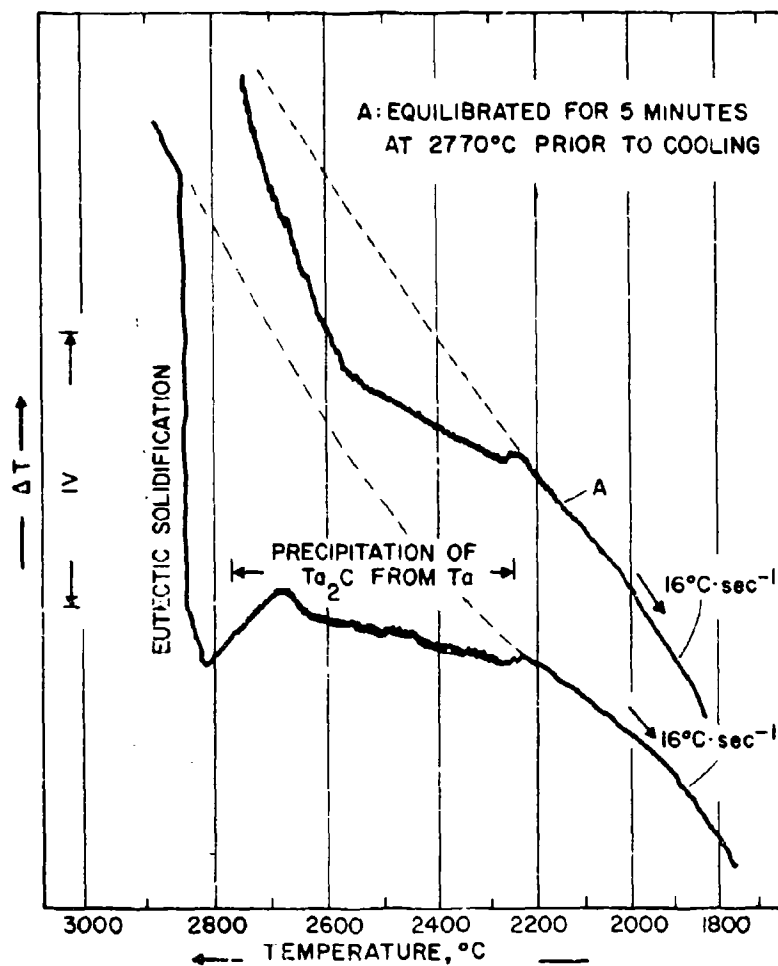


Figure 8. Differential Cooling Curves of a Tantalum-Carbon Alloy with 8 Atomic % Carbon.

thermograms further show, that the bulk of the precipitation occurs at slightly subsolidus temperatures, and is essentially completed at 2200°C. The precipitation of Ta_2C from the tantalum in alloys with more than 3 atomic % carbon proceeds with high speed, and could not be suppressed by quenching with cooling rates up to approximately 1000°C per second.

Examination of the microstructures of quenched specimens showed an essentially random distribution of the Ta_2C precipitates in the tantalum matrix, and a marked tendency for the carbide phase to diffuse to and agglomerate at the grain boundaries of the metal phase (Figures 9, 10, and 11). Precipitate colonies within the matrix grain showing a more or less regular orientation pattern of the carbide grains were occasionally



Figure 9. Ta-C (4 At% C), Cooled at Approximately $40^{\circ}C \text{ sec}^{-1}$ X400 From $2900^{\circ}C$.

Tantalum (Dark) with Ta_2C Precipitates (Light Phase)

Note Precipitate - Depleted Diffusion Zone and Agglomeration of Ta_2C at the Grain Boundaries of the Metal Phase.

noticed in slower cooled ($<10^{\circ}C \text{ sec}$) samples; however, no systematism regarding details in their formation, as well as the orientation of these precipitates relative to the matrix grain could be detected.

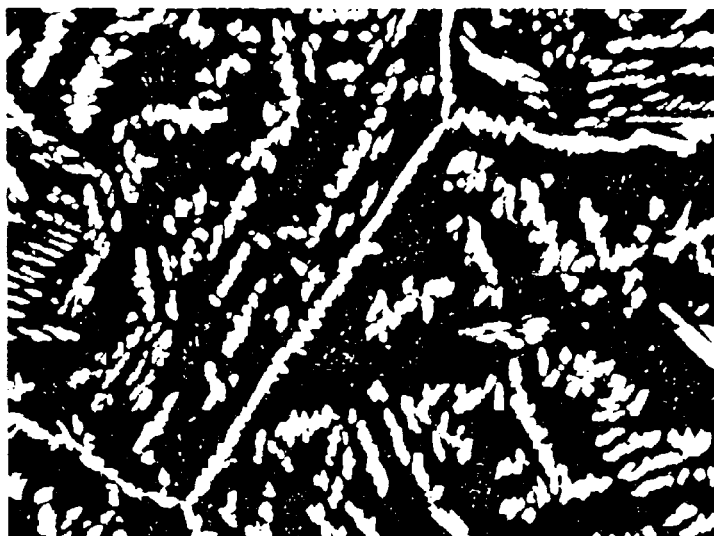


Figure 10. Ta-C (7 At% C), Pre-equilibrated at 2800°C, X250
Cooled with 4°C sec⁻¹ to 2500°C, and Quenched
(100° sec⁻¹).

Tantalum (Dark) With Primary (Light, Large Crystals)
and Secondary (Light, Small Crystals) Ta₂C Precipitates.

In alloys with carbon concentrations of 4, 6, and 7 At%, which were quenched from temperatures slightly above the eutectic line, no eutectic was present, and the micrographs showed the typical precipitation structure. An alloy with 8 atomic % carbon equilibrated and quenched under similar conditions, already contains 20-30% eutectic (Figure 14). On the basis of the metallographic evidence, a maximum solid solubility of 7.5 atomic % carbon at the temperature of the Ta-Ta₂C eutectic was assumed.

b. The Concentration Range up to 25 Atomic % Carbon

Alloys from the concentration range from 8 to 25 At% were two-phased and contained Ta and Ta_2C in varying amounts; the metal-rich (Ta + Ta_2C) eutectic is located at 12 At% C (Figure 15 and 16). Melting of the alloys becomes increasingly two-phased (Table 5) as the carbon concentration of the alloys increases. The metal-rich homogeneity limit of the Ta_2C -phase at the Ta- Ta_2C eutectic temperature is located close to 26 At% C, as evidenced by the micrographs of

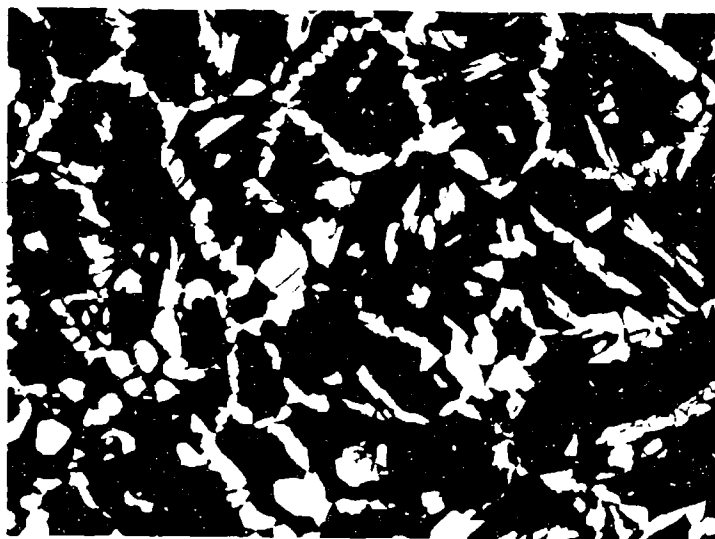


Figure 11. Ta-C (8 At% C), Pre-equilibrated at 2840°C, Cooled with 4°C sec⁻¹ to 2200°C, and Quenched (100°C sec⁻¹)
Dark: Tantalum Phase
Light Equiaxed Crystals: Second Phase Ta_2C
Light Network: Primary (2840 to 2000°C) Ta_2C Precipitates, Agglomerated at the Grain Boundaries.

Light, Small Grains: Rest-Precipitates of Ta_2C From Ta (<2200°C).

alloys with analyzed carbon contents of 25.5 and 26 atomic percent (Figures 17 and 18).

Table 5. Melting Temperatures of Tantalum-Carbon Alloys

Atomic%Carbon				Melting Temp. °C		No. of runs	Cond.	X-Ray		Melting
No.	Nom	Anal	X-Ray*	Incipient	Collapse			Phases	Param.	
1	6			2890	2901	1	1			Slightly Heterog.
2	8			2860	2880	1	1			Slightly Heterog.
3	9			2860	2870	1	1			Slightly Heterog.
4	12	13.0		2840+10	2840+10	4	2			Sharp
5	13			2845	2850	1	1			Sharp
6	16			2850	2891	1	1	$\alpha + \beta$		Slightly Heterog.
7	24			2880	2936	1	2	$\beta + \alpha$	$a=3.101$ $c=4.923$ } β	Very Heterog.
8	26			2940+50	3158+10	2	2	$\beta + \alpha$	$a=3.101$ $c=4.936$ } β	Very Heterog.
9	27	26.7		3040	3297	1	1	$\beta + \alpha$		Very Heterog.
10	28			3048	3307	1	1	$\beta + \text{trace } \alpha$		Very Heterog.
11	29	29.7		3188+50	3323+5	2	1	$\beta + \text{trace } \alpha$		Very Heterog.
12	30	29.2		3240	3369	1	1	β		Very Heterog.
13	31			3265+12	3312+14	2	2	β		Very Heterog.
14	32			3290	3338	1	2	$\beta + \text{tr. } \delta + \alpha$		Very Heterog.
15	33	33.1		3350+15	3440	1	1	$\beta + \text{tr. } \delta$		Very Heterog.
16	34			3360+10	3442+10	2	2	$\beta + \delta$		Very Heterog.
17	35			3350+25	3466+20	2	2	$\beta + \delta$		Very Heterog.
18	36			3420+25	3570+50	1	1	$\beta + \delta$		Very Heterog.
19	37			3400+50	3650+50	2	2	$\delta + \beta$		Very Heterog.
20	38	38.2		3480+50	3720+30	2	2	$\delta + \beta + \text{tr. } \zeta$		Very Heterog.
21	38.5			3490+50		2	2			Very Heterog.
22	39.2			3540+60	3680+10	2	2	$\delta + \beta + \text{tr. } \zeta$		Very Heterog.
23	39.0	38.8		3500+50	3740+20	2	2	$\delta + \beta + \text{tr. } \zeta$		Very Heterog.
24	40			3520+30	3740+25	4	1, 2	$\delta + \beta$		Very Heterog.
25	41			3590+15	3743+6	2	1	$\delta + \text{tr. } \beta + \zeta$		Very Heterog.
26	42	41.6		3700+20	3775+15	2	1	$\delta + \text{tr. } \zeta$		Very Heterog.
27	43		43	3740+30	3800+10	3	1, 2	δ	$a=4.416(a)$	Very Heterog.
28	44		43.8	3705+15	3804+10	4	1, 2	δ	$a=4.420(a)$	Very Heterog.
29	45	44	44.8	3880+25	3900+10	3	1, 2	δ	$a=4.425_8(a)$	Slightly Heterog.
30	46	46.5	45.9	3935+5	3935+5	2	2	δ	$a=4.431_7(a)$	Sharp
31	47	46.7	46.8	3983+15	3983+15	2	2	δ	$a=4.437_1(a)$	Sharp
32	48		48.1	3939+15	3939+15	2	2	δ	$a=4.443_9(a)$	Sharp
33	49		49	3842+10	3842+10	2	2	δ	$a=4.449(a)$	Sharp
34	50			3700+80	3796+15	4	2	δ	$a=4.454_1(a)$	Slightly Heterog.
35	55	57.7		3445+4	3486+20	2	2	$\delta + C$	$a=4.452_d(a)$	Slightly Heterog.
36	60	58.0		3446+0	3446+0	2	2	$\delta + C$	$a=4.454_4(a)$	Sharp
37	65	62.8	49.8	3445+5	>3470	3	2	$\delta + C$	$a=4.453_1(a)$	Heterogeneous

Legend Conditions: 1: 1.1 atm He,

2: 2.3 atm He, 5 cfm He-flow

 α : Tantalum β : Ta₂C-phase δ : TaC-phase

*From lattice parameter of the B1-phase (Bound Carbon)

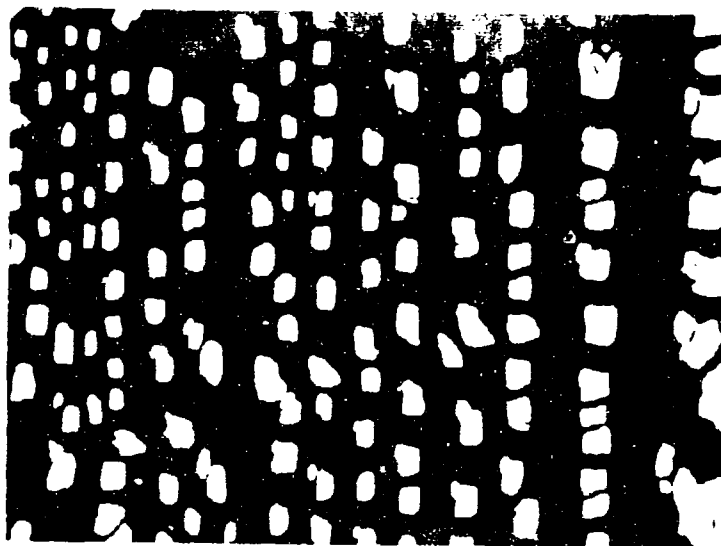


Figure 12. Ta-C (6 At% C), Cooled at Approximately $1^{\circ}\text{C sec}^{-1}$ X1000
from 2800°C .

Colony of Ta_2C -Precipitates (Light) in Tantalum (Dark)

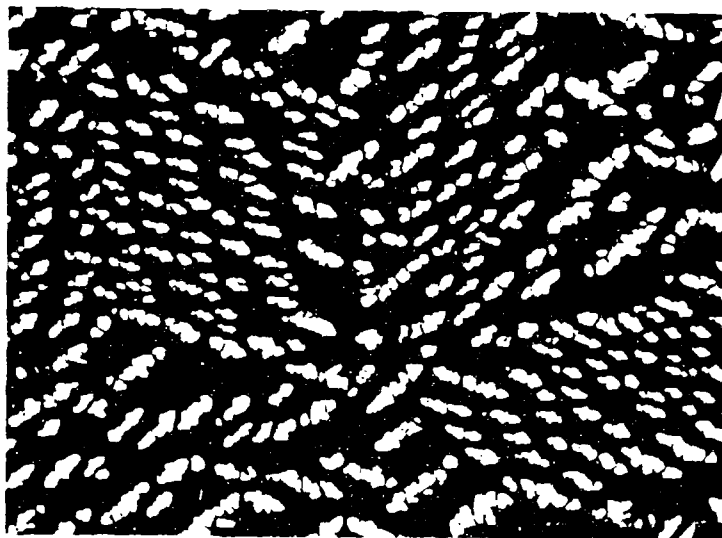


Figure 13. Ta-C (8 At% C), Cooled at Approximately $4^{\circ}\text{C sec}^{-1}$ X400
from 2800°C .

Colonies of Ta_2C Precipitates (Light) in Tantalum (Dark)

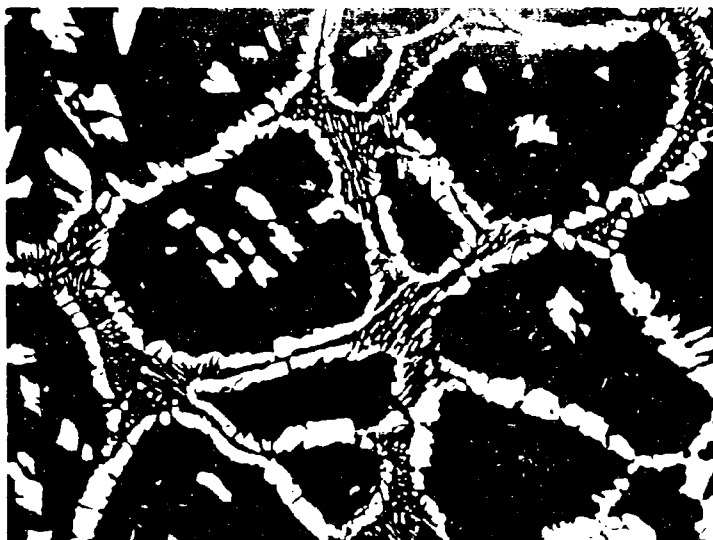


Figure 14. Ta-C (8 At% C), Quenched from 2870°C
 Tantalum Solid Solution with Intragranular Ta₂C
 Precipitates in a Matrix of Ta + Ta₂C Eutectic.

X400



Figure 15. Ta-C (12 At% C), Quenched from 2850°C
 Ta + Ta₂C Eutectic

X250

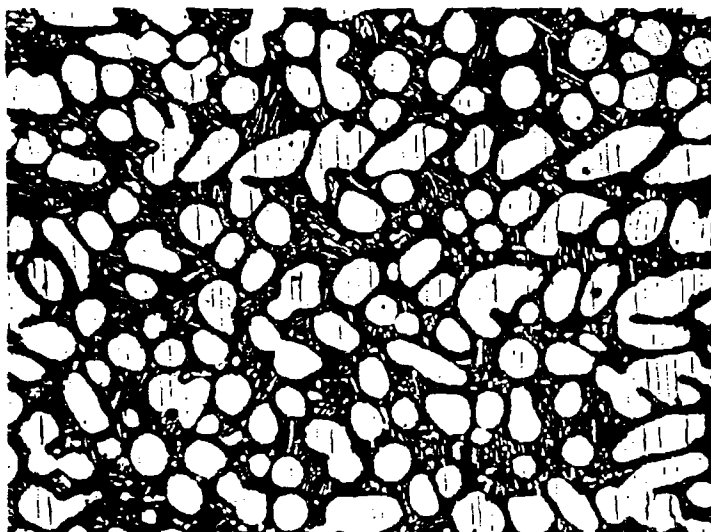


Figure 16. Ta-C (17 At% C), Cooled at $16^{\circ}C \text{ sec}^{-1}$ X90
 Primary Crystallized Ta_2C in a Matrix of $Ta + Ta_2C$
 Eutectic

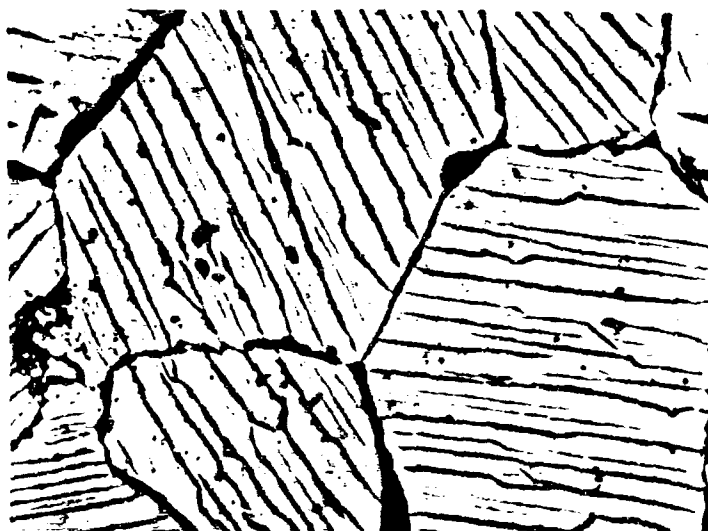


Figure 17. Ta-C (25.5 At% C), Quenched from $2860^{\circ}C$ X750
 Ta_2C with Intragranular Metal Phase Precipitations
 and Traces of Tantalum (Ta_2C -Depleted Eutectic) at
 the Grain Boundaries.



Figure 18. Ta-C (26 At% C), Quenched from 2870°C X750

Originally Single Phase Ta_2C , with Intragranular Tantalum Precipitation Formed During Cooling.

- c. The Concentration Range 25-42 Atomic %
Carbon: α - and β - Ta_2C , and Brauer's ζ -Phase
Starting with approximately 26 atomic percent

carbon, the incipient melting temperatures of the alloys (Table 5, Figure 19) show a sharp increase, reaching in the order of 3300°C at carbon concentrations between 32 and 36 At% C. Melting is in all instances two-phased. This behavior indicates incongruent melting of Ta_2C . X-ray examination of the molten sections of the melting point specimens in the as-quenched state ($\sim 80^\circ\text{C}/\text{sec}$) showed, (Table 5), that the first trace of monocarbide appeared in the samples which were quenched from temperatures above 3300°C. This temperature, therefore, may be taken as the peritectic decomposition temperature of Ta_2C .

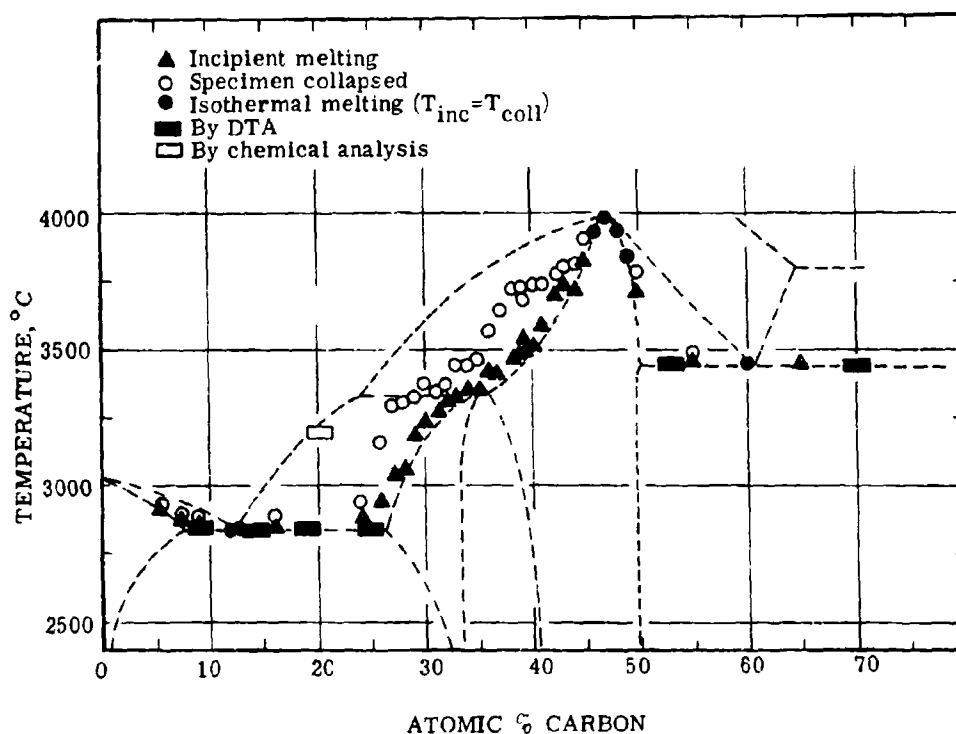


Figure 19. Melting Temperatures of Tantalum-Carbon Alloys

Differential-thermoanalytical investigations performed on Ta_2C -containing alloys showed an interesting behavior: in addition to the thermal arrest associated with the $Ta + Ta_2C$ eutectic reaction isotherm, a sharp and rate-independent thermal arrest is observed at temperatures in the vicinity of $2000^\circ C$ (Figure 20). At substoichiometric compositions the reaction onset on the heating cycle remains fairly constant, but increases sharply to approximately $2200^\circ C$ at stoichiometric compositions (Figures 21 through 24). The temperatures for the thermal arrest again drop to lower temperatures ($\sim 2000^\circ C$) in excess monocarbide-containing alloys

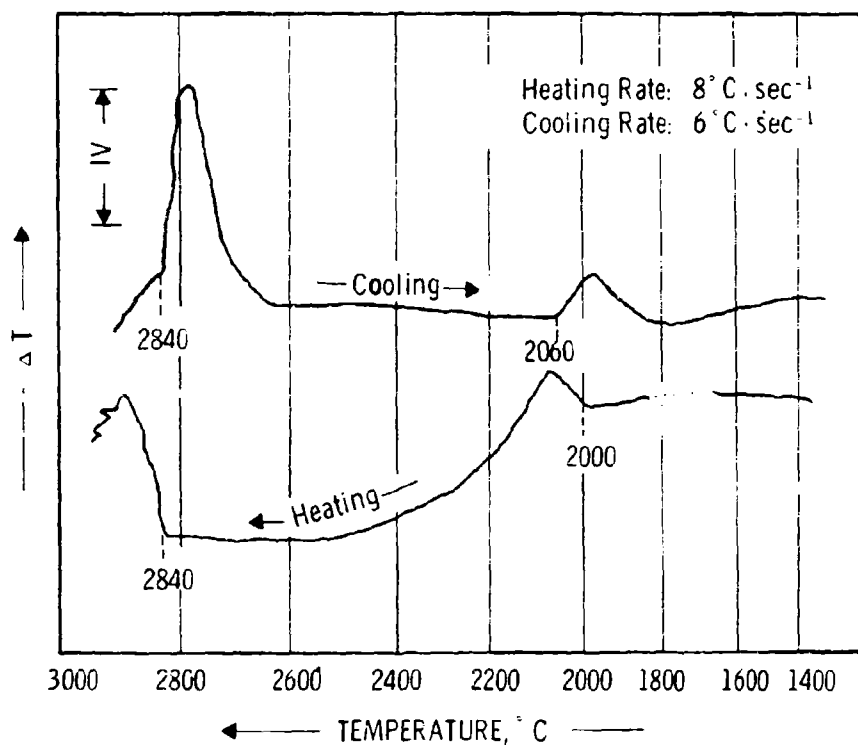


Figure 20. DTA-Thermogram of Tantalum-Carbon Alloy With 21 Atomic % Carbon.

(Figure 25 through 27). The observed thermal arrests are definitely associated with the Ta_2C -phase, since the corresponding peaks on the DTA-thermograms gradually disappear with decreasing contents of Ta_2C (Figure 28).

From thermodynamic considerations, one would assume, that on the heating cycle, the reaction would appear shifted to somewhat higher temperatures than the equilibrium temperature, while the opposite would be expected on the cooling cycle. Prior experience has confirmed these considerations. However, just the contrary is

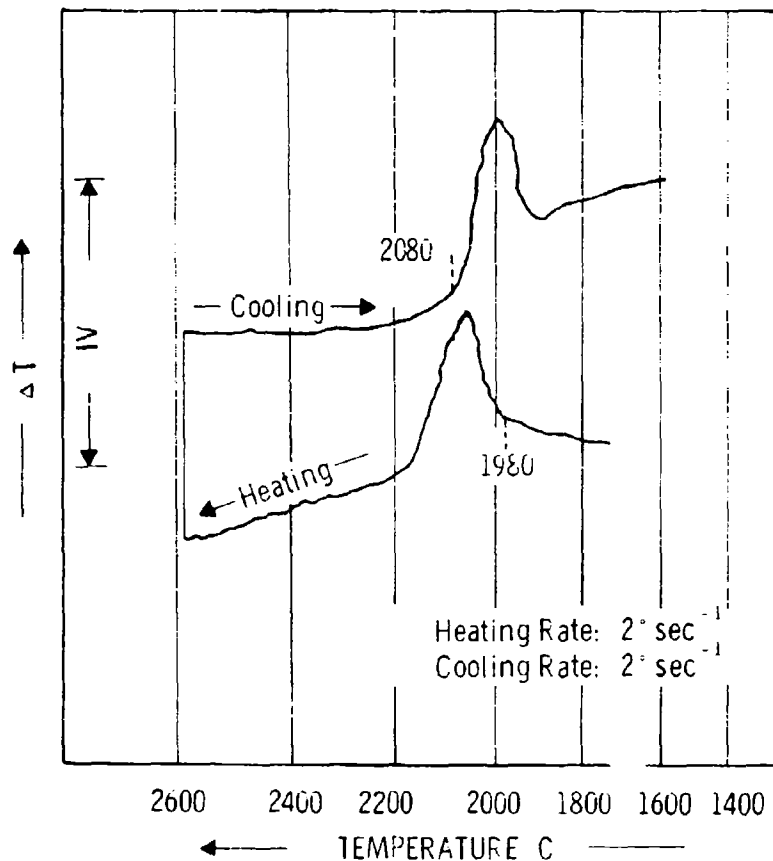


Figure 21. Differential Heating and Cooling Curve of a
Tantalum-Carbon Alloy with 30 Atomic % Carbon
(Inverted ΔT -Signs on Heating and Cooling Cycles)

observed in the present case, i.e. the reaction initiates at higher temperatures on the cooling cycle than on the heating cycle, although a somewhat closer inspection of the peaks reveals a considerable overlap or almost a coincidence of the temperatures of the maximum enthalpy change.

This reaction behavior becomes explainable, if a two-phased reaction (transformation) process for Ta_2C is assumed, i.e. that a two-phase field is passed as the temperature range of the

transformation is traversed in the experiment. The reaction onset on the heating cycle then would correspond to crossing the eutectoid line (lowest temperature of stability for the high temperature modification), whereas the initiation of the thermal arrest on the cooling cycle (upper

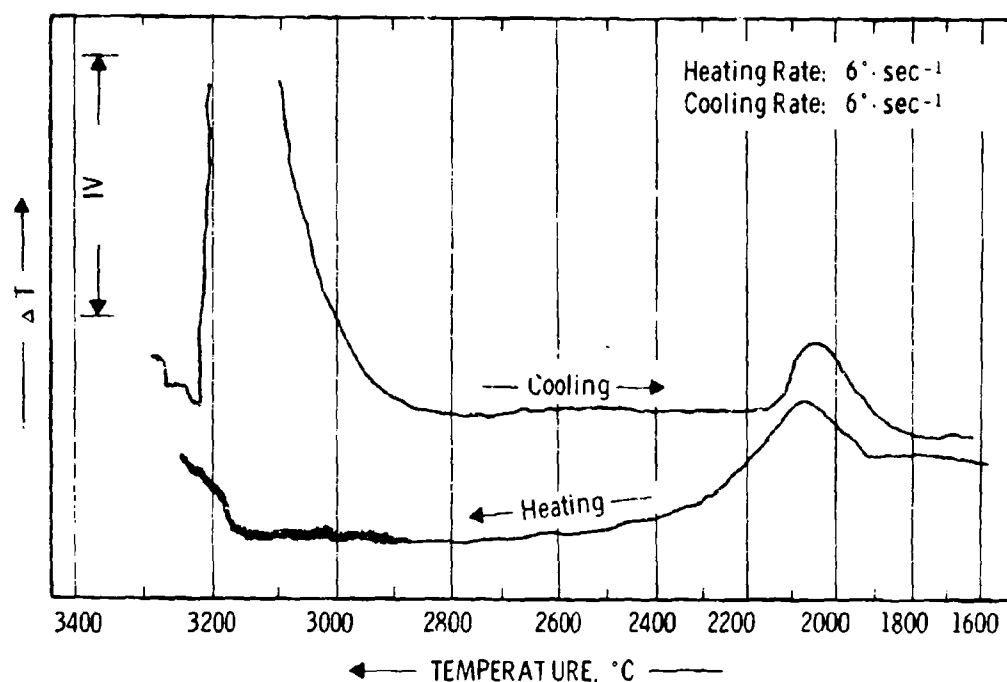


Figure 22. Differential Heating and Cooling Curve of a Tantalum-Carbon Alloy with 32 Atomic % Carbon. (Inverted ΔT -Signs on Heating and Cooling Cycles)

Note: To Preserve Sample Geometry the Experiment was Stopped After Incipient Melting was Noted.

temperature stability limit of the low temperature modification) would correspond to passing the peritectoid line on the metal-rich side of the phase.

The observed shift of the reaction onset with the carbon concentration in excess tantalum-containing alloys must be related to kinetic effects incurred by the simultaneous presence of tantalum, since the homogeneity range of Ta_2C is very small at temperatures below 2200°C.

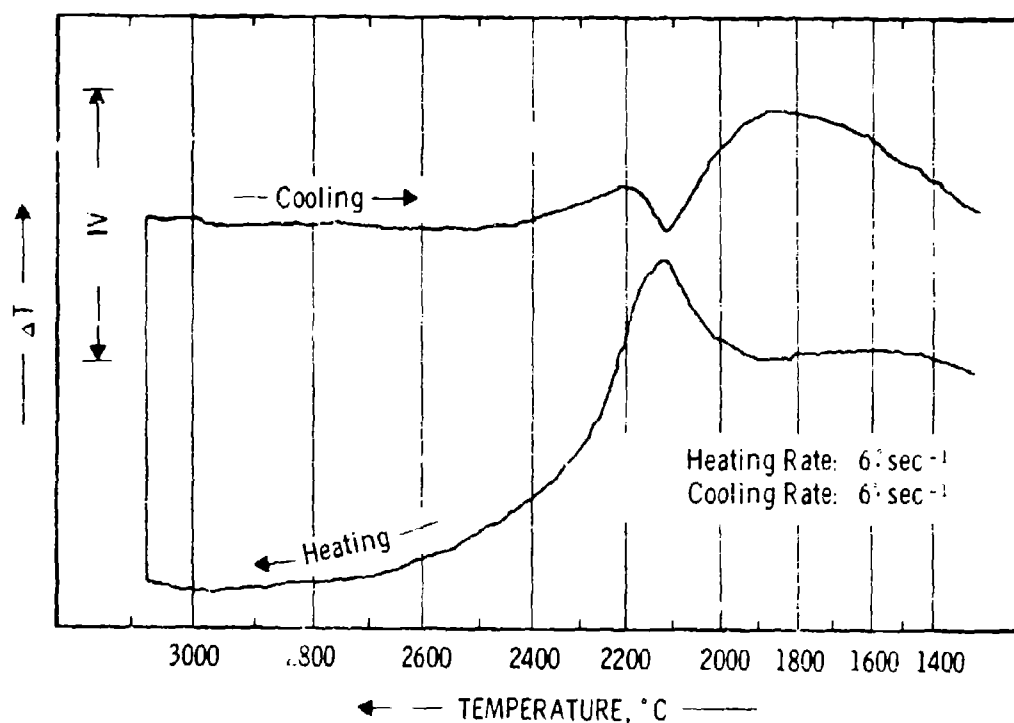


Figure 23. Differential Heating and Cooling Curve of a Tantalum-Carbon Alloy With 33 Atomic % Carbon.

The lattice parameter variations of Ta_2C in long-time heat-treated as well as quenched alloys (Figure 29) were only very nominal in $Ta_2C + Ta$ and $Ta_2C + TaC (+\zeta)$ containing alloys ($a = 3.100$ to 3.102 \AA ; $c = 4.931$ to 4.940 \AA) for alloys heat-treated at 1700°C, (Table 6).

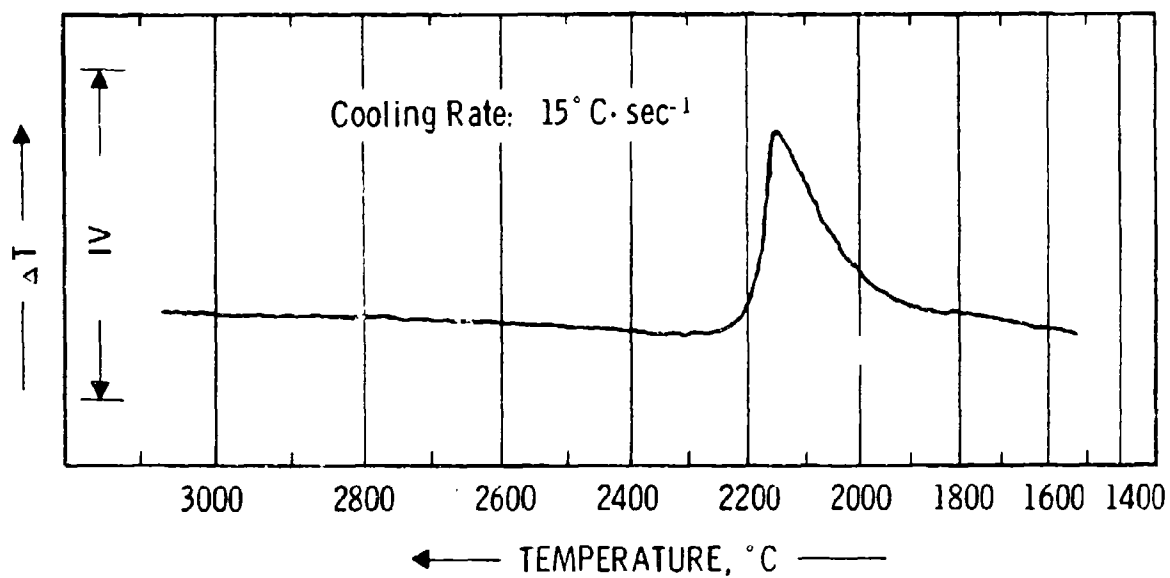


Figure 24. Differential Cooling Curve of a Tantalum-Carbon Alloy with 33 Atomic % Carbon (Rapid Cooling Conditions).

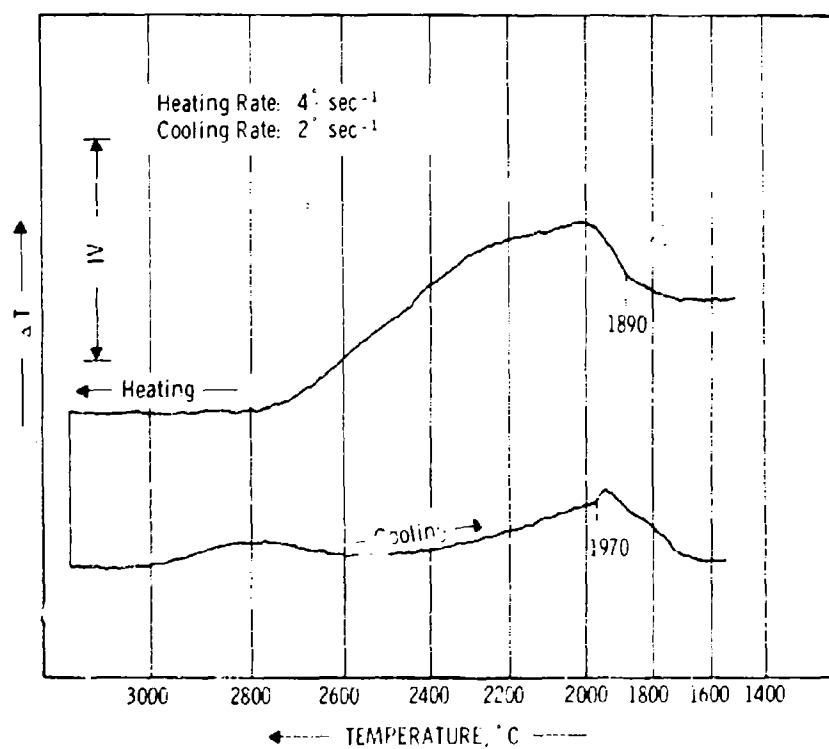


Figure 25. Differential Heating and Cooling Curve of a Tantalum-Carbon Alloy with 36 Atomic % Carbon.

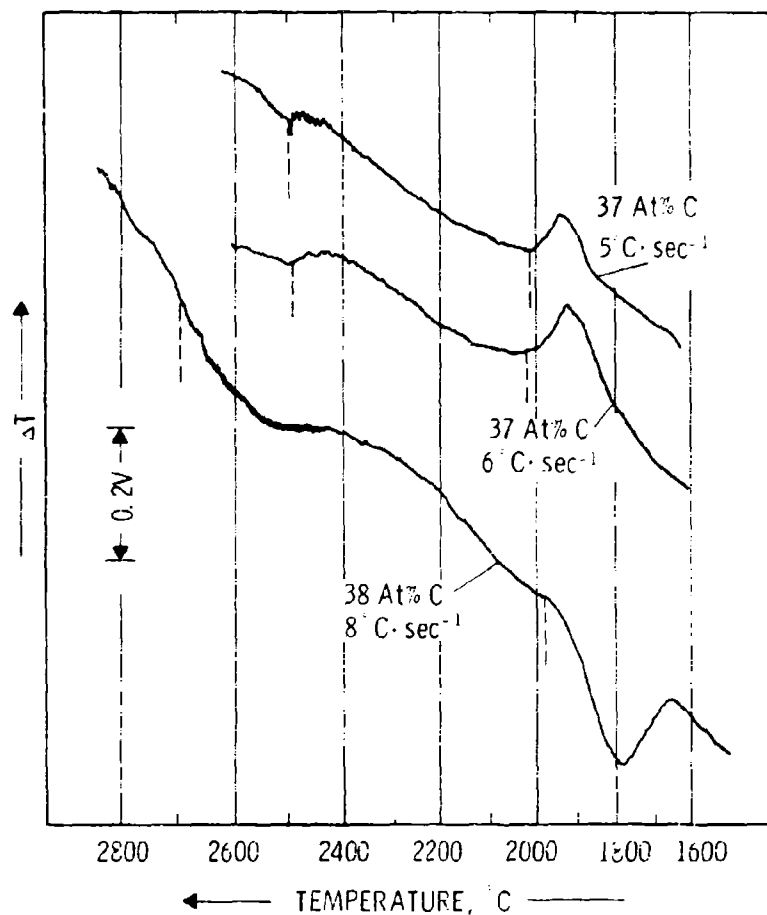


Figure 26. Differential Cooling Curves of Tantalum-Carbon Alloys with 37 and 38 Atomic % Carbon (Inverted ΔT -Sign for 38 At% C Curve)
(High 'ty Scale)

The largest parameter for the hexagonal close-packed phase was derived from an alloy with 36 atomic percent carbon, which was quenched from 2500°C: $a = 3.107 \text{ \AA}$, $c = 4.947 \text{ \AA}$ (Table 6); this indicates a slight temperature dependence of the carbon-rich boundary towards higher temperatures.

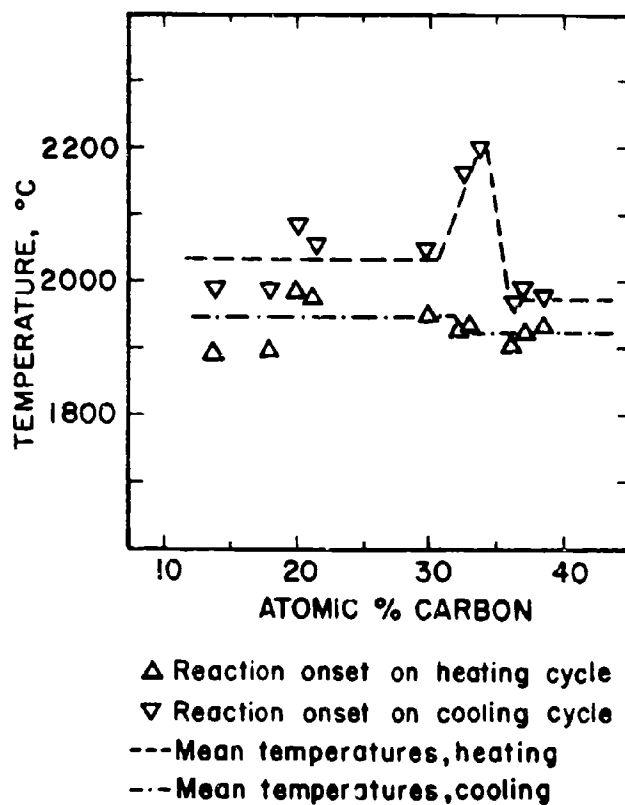


Figure 27. α - β - Ta_2C Phase Reaction as a Function of the Carbon Concentration.

The diffraction lines of the Ta_2C -phase in alloys which were quenched from above 2100°C were very diffuse, while subsequent annealing at lower temperatures (1500 - 1900°C) produced sharp patterns. This observation is certainly related to the phase change of Ta_2C , and the occurrence of diffuse patterns further supports the assumption of a two-phased reaction process.

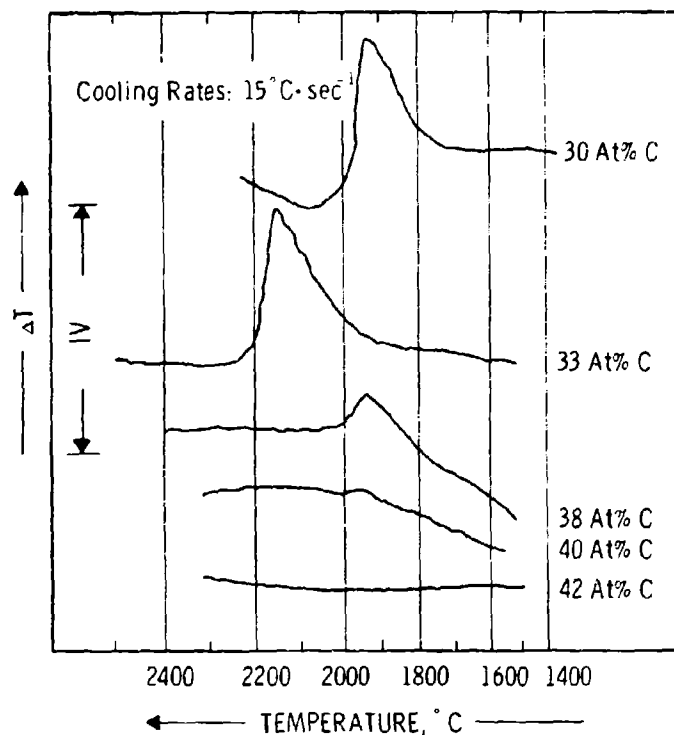


Figure 28. α - β - Ta_2C Reaction Under Rapid Cooling Conditions: Differential Cooling Curves of Alloys in the Range From 30 to 42 Atomic % Carbon.

No signs for a structurally different phase were found in rapid quenching studies performed with cooling speeds between approximately 500 and 2000°C per second. Therefore, the α - β - Ta_2C phase reaction either has to proceed with extremely high speed, proceeding to completion under the chosen cooling conditions, or the transformation process does not involve a structural change of the metal host lattice, but merely affects the distribution of the carbon atoms in the octahedral interstices of the hexagonal close-packed framework of the metal atoms. The experimental evidence is in favor of the latter assumption.

Table 6. Lattice Parameters of Ta₂C

Gross Composition At% C	Heat Treatment	Phases Present (X-Ray)	Lattice Parameters λ Me ₂ C-Phase	
			a	b
16	2840 ↓	β + α	3.101	4.923
26.7	3200 ↓	β + α	3.101	4.936
33.1	~3000 ↓	β + trace δ	3.105	4.942
18	50 hrs, 1500°C, 10 ⁻⁵ Torr	β + α	3.100	4.930
33.3	8 1/2 hrs, 2200°C, 10 ⁻⁵ Torr	β + trace δ	3.103	4.938
33.3	64 hrs, 1520°C, 10 ⁻⁵ Torr	β + trace δ	3.100	4.938
33.5	7 min, 2200°C ↓	β + trace δ	3.103	4.935
33.5	5 min, 2500°C ↓	β + δ	3.101	4.937
32.0	225 hrs, 1600°C, 10 ⁻⁵ Torr	β	3.100	4.936
36.4	9 hrs, 1750°C, 10 ⁻⁴ Torr	β + δ	n.d.	n.d.
37.4	12 min, 2200°C ↓	β + δ	3.105	4.946
36.2	7 min, 2500°C ↓	β + δ	3.107	4.947
37.2	12 min, 2200°C ↓	β + δ	3.106	4.944
37.4	7 min, 2500°C ↓	β + δ	3.106	4.941
37.2	7 min, 2200°C, +24 hrs, 1700°C, 10 ⁻⁵ Torr	β + δ + ζ	3.101	4.942
36.2	7 min, 2200°C, +24 hrs, 1700°C, 10 ⁻⁵ Torr	β + δ + trace ζ	3.104	4.941

Legend to Table 6.

↓ : Rapidly quenched in tin
n.d.: not determined

Due to experimental difficulties, no direct proof could be obtained by high temperature X-ray diffraction experiments. There is, however, sufficient indirect evidence, such as the formation of a complete series of solid solutions between Ta_2C and W_2C at high temperatures⁽⁴¹⁾, that the α - β - Ta_2C phase reaction does not affect the basic structure of the metal frame work. This supposition is further strengthened by the fact, that a related case has been found in Mo_2C ⁽⁵⁾, where the reaction is slow enough to allow the β -modification to be frozen in by rapid quenching.

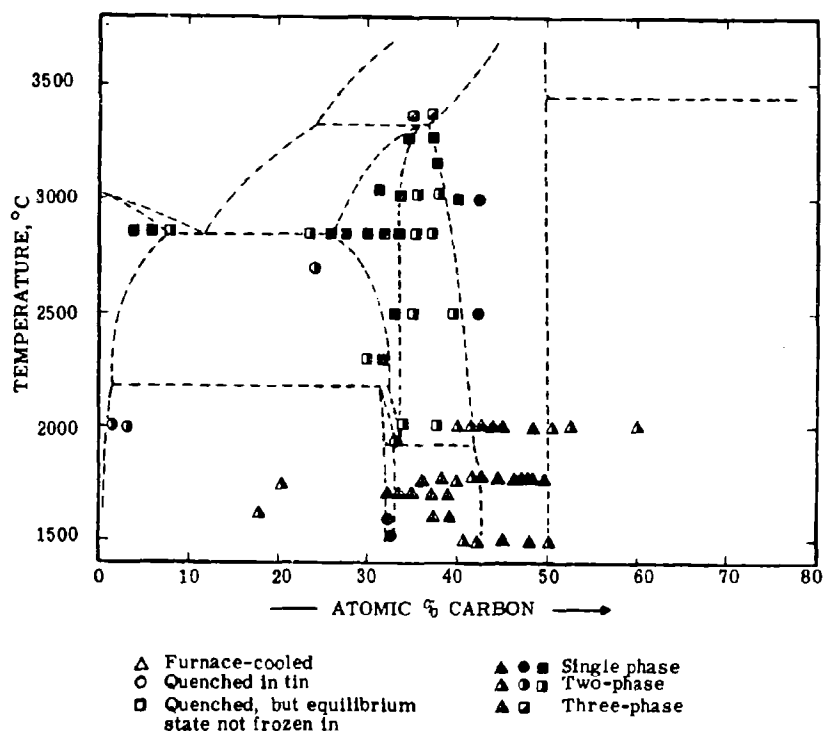


Figure 29. Tantalum-Carbon: Position and Qualitative X-Ray Evaluation of the Alloys for the Investigation of the Solid State Portion of the System.

The main interest at this point now concentrates on the effect of the α - β - Ta_2C phase reaction on the appearance of the microstructures, and we would expect to obtain some additional evidence, especially pertaining to the question whether the transformation proceeds as a homogeneous or a two-phased process.



Figure 30. Ta-C (30 At% C) Rapidly Cooled ($40^\circ\text{C sec}^{-1}$) X1000
From 3380°C .

Nonequilibrium Structure Consisting of Ta_2C , Ta and TaC_{1-x} .

A problem in the study of the alloys in the critical concentration range from 33 to 36 At% C consisted in obtaining dense enough bodies and with sufficiently large grains for the metallographic examination. This generally required, that the samples had to be partially

or completely molten. Two alloy series, one prepared by arc melting and the other by equilibration of alloys above solidus temperatures, initially lead to partially erroneous conclusions regarding the high carbon boundary of the Ta_2C phase. The arc molten alloys usually showed severe phase segregations, while in the alloys equilibrated above solidus, the peritectic reaction did not proceed to completion during rapid cooling. Both methods yielded nonequilibrium structures (Figure 30), which could not be corrected in feasible lengths of time by equilibration treatments at lower (1700 - 2200°C) temperatures.

In order to circumvent these difficulties, diffusion-couple experiments, analogous to those described by G. Santoro and H. B. Probst⁽¹¹⁾ for this alloy system, were performed. The Ta-C diffusion couples were prepared by resistively heating a thin (~ 3 mm) tantalum rod between two copper-cooled electrodes to temperatures of 2000 to 2300°C. High purity methane was admitted to the furnace chamber in a quantity sufficient to produce a 1 mm deposit of pyrolytic graphite on the sample substrate. The temperature measurements were carried out pyro-optically on a black body hole of approximately 0.5 mm diameter drilled into the pyrolytic graphite deposit. The graphite was then allowed to diffuse into the tantalum.

A second set of diffusion experiments was carried out by holding tantalum-carbon samples of varying carbon content in graphite containers above the temperature of the Ta- Ta_2C eutectic. The objective of the second experiment series was two-fold: First to extend the studies regarding the behavior of the

Ta₂C-TaC boundary at temperatures close to the peritectic, and second to obtain data for the subcarbide-saturated liquidus.

Examination of alloys from the concentration range 26 to 30 At% C (Figure 18), which were quenched from temperatures above the eutectic line, showed Ta₂C with the typical unidirectional tantalum precipitations. In each instance ($\leq 500^\circ\text{C sec}^{-1}$) precipitation of tantalum from the originally homogeneous Ta₂C proceeded to an extent, that at low temperatures a Ta₂C-phase with an approximate carbon content of 30-31 atomic percent resulted. The appearance of the microstructure at the higher carbon concentration undergoes a certain change inasmuch, as in addition to the tantalum precipitation, a faint substructure seems to become visible (Figure 31).

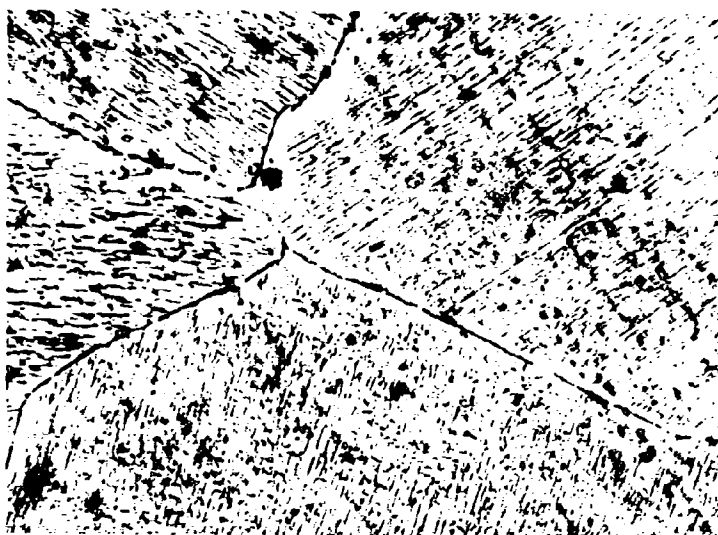


Figure 31. Ta-C (29 At% C), Quenched from 3050°C. X750
Ta₂C With Unidirectional Ta-Precipitations and a Possible Additional Substructure.

Typical results from the diffusion experiments are presented in Figures 32 through 34. Sharp boundaries were observed between the excess tantalum-containing portion and Ta_2C , as well as between Ta_2C and the monocarbide phase, both show a low carbon phase boundary (Figures 33 and 34). The amount of tantalum precipitation upon cooling decreases with increasing carbon content, as evidenced by the decreasing width of the dark precipitates shown in Figure 34. Equilibration experiments carried out between 3100 to 3300°C indicate a sharp increase of the high carbon boundary of the Ta_2C phase in this temperature range (Figure 35). Within any given grain, the TaC -precipitations are unidirectional. In view of the nearly identical atomic arrangement and occupational densities, it is to be assumed, that the (111) phase of the monocarbide grows epitaxially on the basal plane of Ta_2C upon cooling.

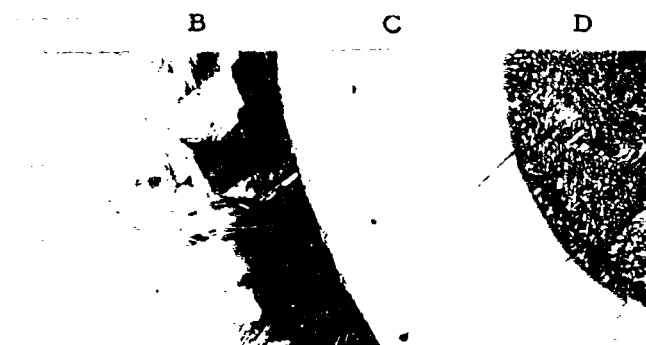
Chemical analysis results of the center portion of the Ta-C diffusion couples, representative of the composition of the liquidus in equilibrium with the subcarbide phase at the chosen equilibrium temperatures, are presented in Table 7.

Microscopic examination of the Ta_2C -phase layers under vertical illumination revealed the presence of a substructure such as shown in Figures 36 and 37. The same type of substructure was observed without exception in each subcarbide grain. Although less characteristic than in the corresponding case with molybdenum^(5, 42), the structure has a certain resemblance to the transformation patterns observed in Mo_2C and W_2C ⁽⁴²⁾, thus suggesting a two-phased reaction process. The volume of the new phases (β - Ta_2C on the heating cycle, and α - Ta_2C on the



a. X25

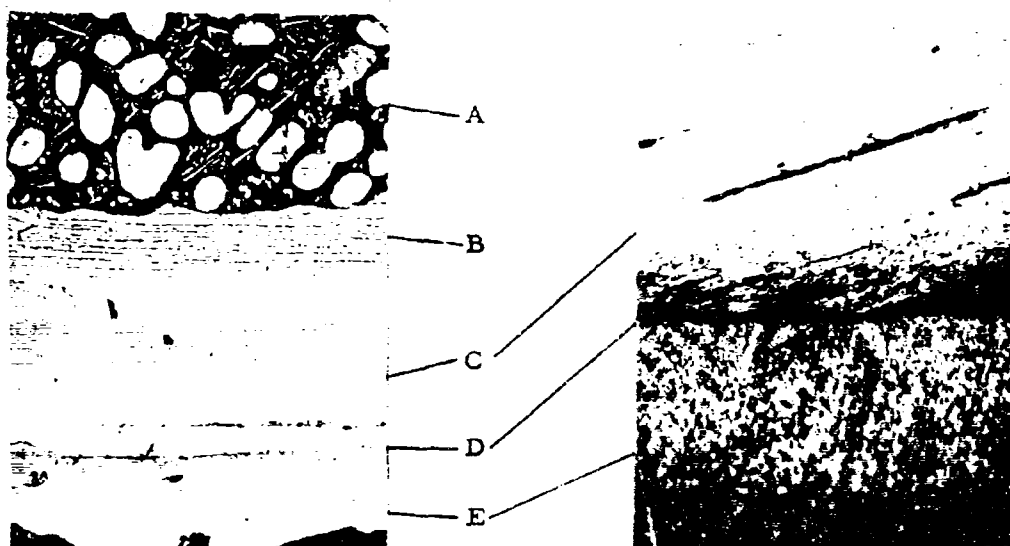
A B C D C B A



b. X70

Figure 32 a & b. Tantalum-Carbon Diffusion Couple,
(1 hr at 2850°C) With Knopp Hardness
Indentations .

- A: Monocarbide
- B: Monocarbide with Precipitations($\zeta + \text{Ta}_2\text{C}$)
- C: Subcarbide
- D: $\text{Ta} + \text{Ta}_2\text{C}$ Eutectic



a. X90

b. X400

Figure 33 (a & b). Ta-C Diffusion Couple, 15 min at 3000°C
(Cooled at 14°C per Second.

- a:
- A: Primary Ta_2C , and Ta + Ta_2C Eutectic. Overall Composition $16 \pm 1.5 \text{ At\% C}$.
 - B: Ta_2C With Unidirectional Tantalum Precipitations
 - C: Ta_2C
 - D: Ta_2C With Monocarbide Precipitation
 - E: Tantalum Monocarbide
- b:
- Interface Between Ta_2C -TaC at Higher Magnification.



Figure 34. Ta-C: Diffusion Couple Shown in Figure 32; X400
Enlargement of the Ta_2C -Liquid Interface.

Note Decreasing Amount of Ta-Precipitation (Dark)
with Increasing Carbon Concentrations.

cooling cycle, respectively), grows at the expense of the other. Considering the type of transition, we may speculate, that it is characterized by the destruction of long range order (2nd order transition) in the carbon sublattice at the observed transition temperatures.



Figure 35. Ta_2C -C Diffusion Couple, 15 min at 3200°C . X1000
Unidirectional Monocarbide Precipitation in Ta_2C + Trace
Monocarbide. (Vertical Illumination).

Annealing of the alloys proceeds extremely slow and extended heat treatments (> 200 hrs) in the temperature range from 1600 to 1900°C are necessary in order to establish the equilibrium conditions at this temperature.

The unidirectional (monocarbide) precipitations in Ta_2C , which are evidence for the extension of the carbon-rich phase boundary to hyperstoichiometric composition, are again pronounced in slightly hyperstoichiometric Ta_2C , which was reannealed after quenching from temperatures in excess of 3000°C (Figures 38 through 40).

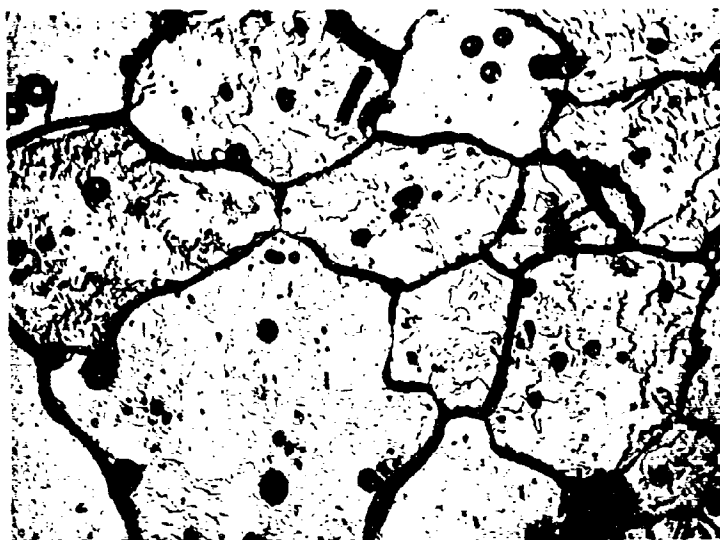


Figure 36. Ta-C: Diffusion Couple

X600

Structure Developed in Ta_2C After Rapid Quenching from 2800°C.

(Vertical Illumination)

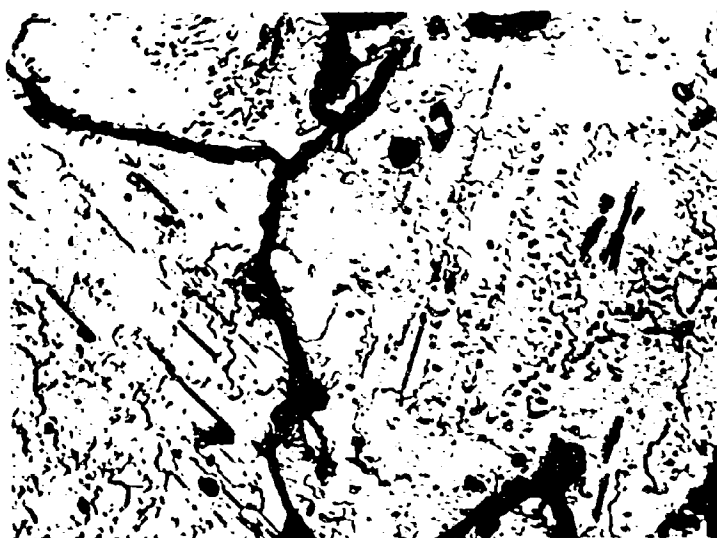


Figure 37. Ta-C: Diffusion Couple

X1000

Sample from Figure 36, Ta_2C Layer Under Higher Magnification.

(Vertical Illumination)

Table 7. Compositions of the Liquidus in Equilibrium with Ta_2C :
Analytical Results from Ta-C Diffusion Couples

Equilibration Temperature °C	Composition of the Core At% C
(2843)	(12)
3000	16 ± 1.5
3100	17 ± 1.5
3200	20 ± 2



Figure 38. Ta-C (~ 34 At% C), Quenched From 3100°C, and Heat-Treated for 24 hrs at 1750°C. X400
 Ta_2C With TaC Precipitation



Figure 39. Ta-C (35 At% C), Quenched From 3250°C,
and Heat-Treated for 225 hrs at 1600°C.

X1000

Coagulated Monocarbide Precipitations in Ta_2C .

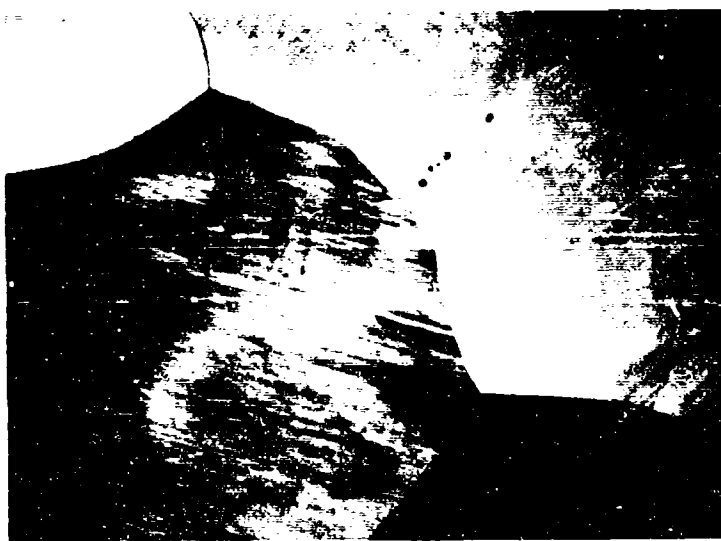


Figure 40. Ta-C (33.3 At% C), Quenched From 3000°C
and Heat-Treated for 225 hrs at 1600°C.

X500

Traces of Localized TaC-Precipitations.

Note Substructure in Grain.

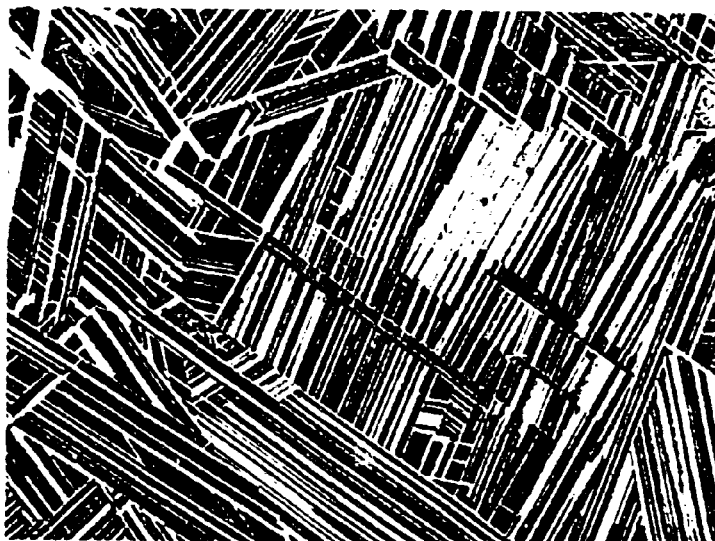


Figure 41. Ta-C (38 At% C), Quenched from 3300°C,
TaC Precipitation Structure.

X250

X-Ray: TaC_{1-x} + Ta_2C + Traces of ζ .

In alloys from the concentration range from 35 to 42 At% C the occurrence of Brauer's ζ -phase was noticed on the X-ray patterns. Despite considerable attempts, which included quenching studies from temperatures up to 3500°C, as well as long-time annealing (25 - 300 hrs) at temperatures varying between 1500 and 2000°C, the phase never could be obtained in pure form. It is interesting to note, that the occurrence of the ζ -phase is dependent on the simultaneous presence of the monocarbide phase while all other combinations of phases, i.e. Ta_2C + TaC, Ta_2C + TaC + ζ , TaC + ζ , were found in the alloy samples, the pair Ta_2C + ζ never was observed.

While alloys with 35, 36 and 37 At% C, which were quenched from temperatures close to the peritectic line, showed primarily Ta_2C and monocarbide, with only traces of ζ -phase present, pure precipitation structures were obtained in samples having carbon concentrations between 38 and 41 atomic percent (Figure 41). X-ray examination of these alloys revealed that in the alloys with 40 and 41 atomic percent carbon only ζ and the monocarbide were present.

Annealing of high temperature (2200 - 2700°C) quenched alloys from the concentration range 36 to 39 At% C resulted in an initial increase of the relative amount of ζ -phase; however, a 400 hr treatment at approximately 1700°C showed a definite decrease. Results of these experiments already indicate that the ζ -phase might be the result of a non-equilibrium precipitation from substoichiometric tantalum monocarbide, and thus does not represent a true equilibrium phase.

Probably the most conclusive evidence for this assumption is given by the diffusion couple experiments, which show that no sharp boundary is formed between the precipitate phase and the monocarbide (Figures 32 and 33). These experiments were in repetition to experiments made by G. Sanboro and H. Probst⁽³⁶⁾, who first outlined this behavior and interpreted it in terms of ζ - as being a non-equilibrium product.

Sectioning of the sample and examining the layers by X-ray diffraction were in confirmation of the previously made assumptions: In the precipitation layer closest to the Ta_2C , the X-ray patterns showed a mixture of Ta_2C , ζ , and TaC_{1-x} , whereas in the area close to the single phase monocarbide zone, only monocarbide and ζ were

present. Finally, the outer layer, which appears as single phase in the micrographs, consisted of monocarbide only. The very outer zones of the diffusion couple was yellow-colored, which is typical for tantalum monocarbide containing more than 46 atomic percent carbon.

The results of the X-ray and metallographic investigation apparently are to be interpreted such, that at temperatures in excess of 2500°C the reaction speeds are sufficiently high, so that the ultimate reaction product is Ta_2C . Precipitation initiating at lower temperatures (in alloys with 40 to 42.5 atomic percent carbon) produces the non-equilibrium precipitate ζ , which grows epitaxially on TaC_{1-x} . Owing to the extreme slow reaction rates prevailing at temperatures below 2000°C, collective recrystallization of the precipitation structure, accompanied by a gradual disappearance of ζ , proceeds very sluggishly. Although in bulk form, thermodynamically instable with regard to a mechanical mixture of sub- and monocarbide, the epitaxial, and hence, structurally closely related may initially have higher stability than Ta_2C precipitates of comparable size.

d. Tantalum Monocarbide

Following the slight inflection in the measured solidus temperatures due to the peritectic decomposition of Ta_2C (Figure 19), the solidus temperatures of the alloys increase rapidly with increasing carbon content (Figure 18 and Table 5). Congruent melting was found at a temperature of 3983°C at carbon concentration of 47 atomic percent. Above the congruently melting composition, the solidus temperatures drop rapidly as the stoichiometric composition is approached.

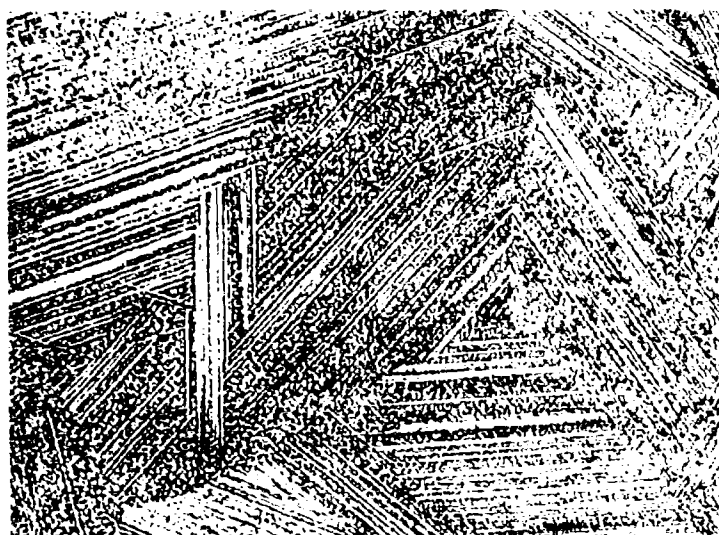


Figure 42. Ta-C (40 At% C), Cooled at $100^{\circ}\text{C sec}^{-1}$ from 3500°C . X250
Monocarbide With Precipitations (ζ).

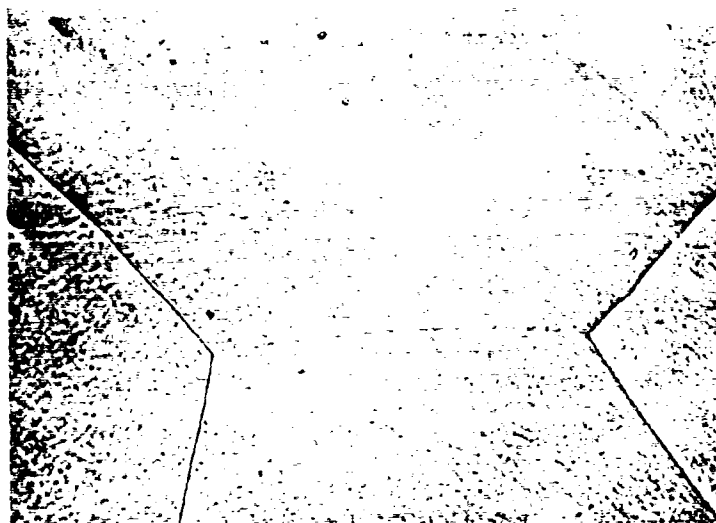


Figure 43. Ta-C (42 At% C), Cooled at $100^{\circ}\text{C sec}^{-1}$ from 3700°C . X700
Single Phase Monocarbide
(Aperture Closed to Reveal Grain Boundaries)

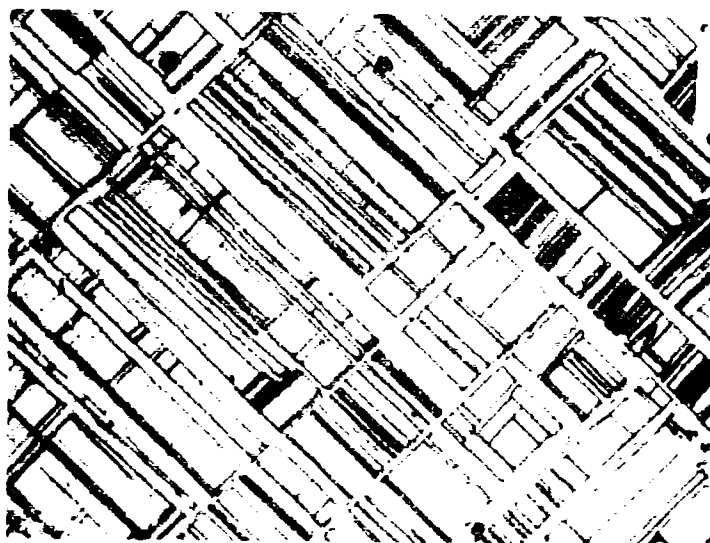


Figure 44. Ta-C (37 At% C), Cooled at $5^{\circ}\text{C sec}^{-1}$ from 3300°C. X1000

Subgrain Structure Developed in Substoichiometric Tantalum Monocarbide.

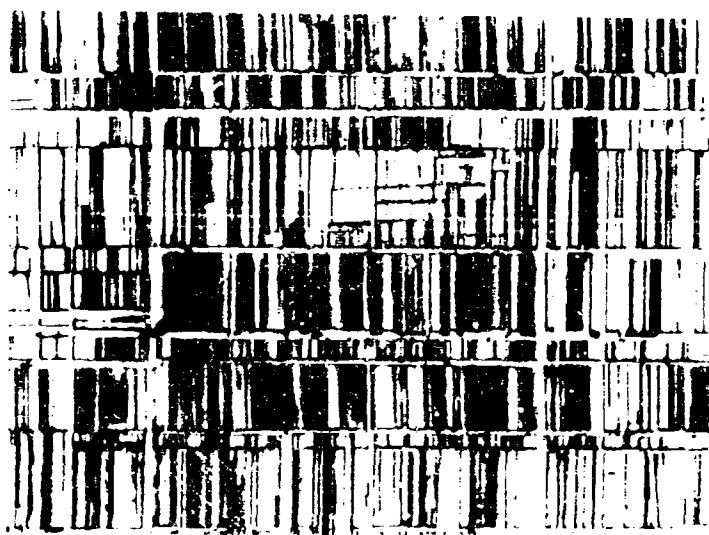


Figure 45. Ta-C (39 At% C), Cooled at $5^{\circ}\text{C sec}^{-1}$ from 3300°C. X1000

Precipitation Structure in Substoichiometric Tantalum Monocarbide.

Metallographic examination of quenched alloys revealed, that precipitation was always present up to total carbon concentrations of 42 atomic % (Figure 42 and 43). The microstructures shown occur, if the bulk of the precipitation reaction is allowed to proceed at high temperatures (slow cooling rates). Annealing of these decomposition structures is extremely slow (Figures 46 and 47), but ultimately results in distinct two-phase structures, which are formed by collective recrystallization.

Alloys from the concentration range 42 to 49.4 At% C, which were quenched from temperatures above 3300°C, are single phase (Figure 48). A sample with 50.2 At% C, quenched from the same temperature (Figure 49), already contained scant traces of excess graphite. The excess graphite already becomes easily recognizable in a specimen with 51.5 At% C, which was prepared under similar conditions (Figure 50).

Apart from the metallographic investigations which indicated at the peritectic line (3330°C) a homogeneity range between 36.5 and ~49.5 At% C, an alloy series was heat-treated at 1700°C and investigated by X-ray diffraction. Bound and free carbon in the heat-treated alloy series were determined analytically. At 1700°C, the monocarbide phase extends from 42.5 At% C ($a = 4.413 \text{ \AA}$) to 49.8 At% C ($a = 4.456 \text{ \AA}$). The lattice parameters vary practically linearly with the carbon content, thus confirming the results by R. Lesser and G. Brauer⁽¹⁵⁾ as well as later redeterminations^(12, 29, 30) (Figure 4).

No indications for a phase change of the monocarbide phase⁽³¹⁾ could be detected metallographically as well as

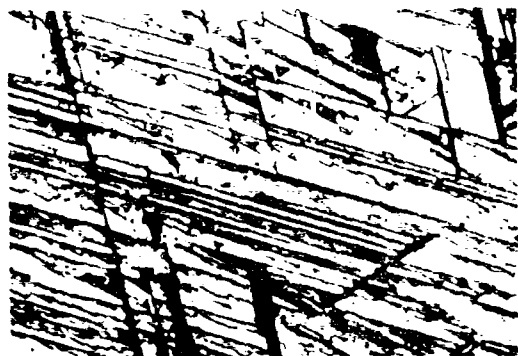


Figure 46. Ta-C (37 At% C), Cooled at $5^{\circ}\text{C sec}^{-1}$
From 3300°C and Heat-Treated for 24 hrs
at 1700°C .

X1000

Collective Recrystallization of the Decomposition
Structure with Formation of Two Distinct Phases.

X-Ray: $\text{Ta}_2\text{C} + \text{TaC}_{1-x} + \text{Trace } \zeta$

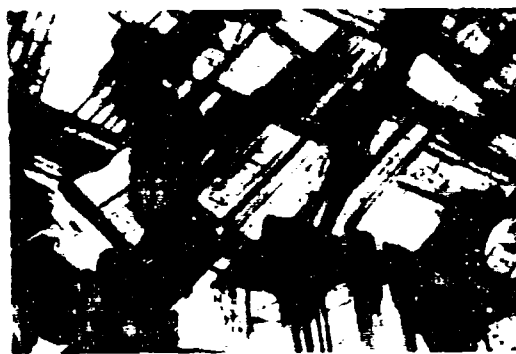


Figure 47. Ta-C (39 At% C), Quenched from 3500°C ,
and Annealed for 24 hrs at 1700°C .

X1000

Subgrain Growth of Ta_2C in Substoichiometric
Tantalum Monocarbide.

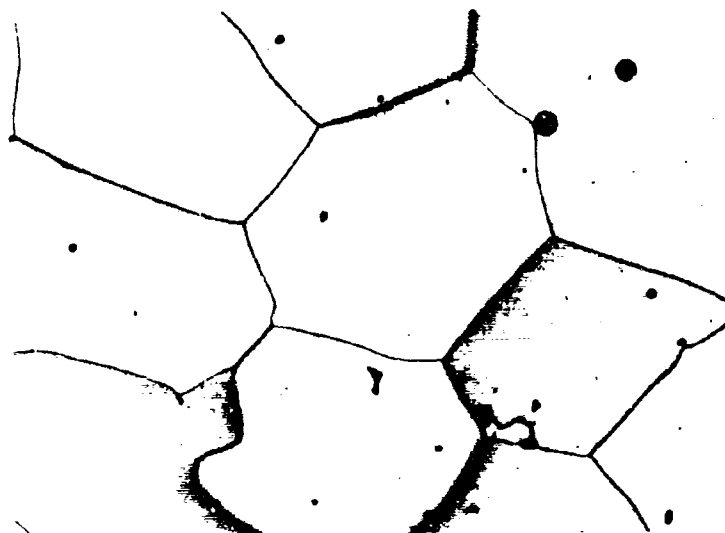


Figure 48. Ta-C (49.3 At% C), Quenched from 3450°C. X200
Single Phase TaC.



Figure 49. Ta-C (50.2 At% C), Quenched from 3500°C. X900
TaC With Traces of Excess Graphite.

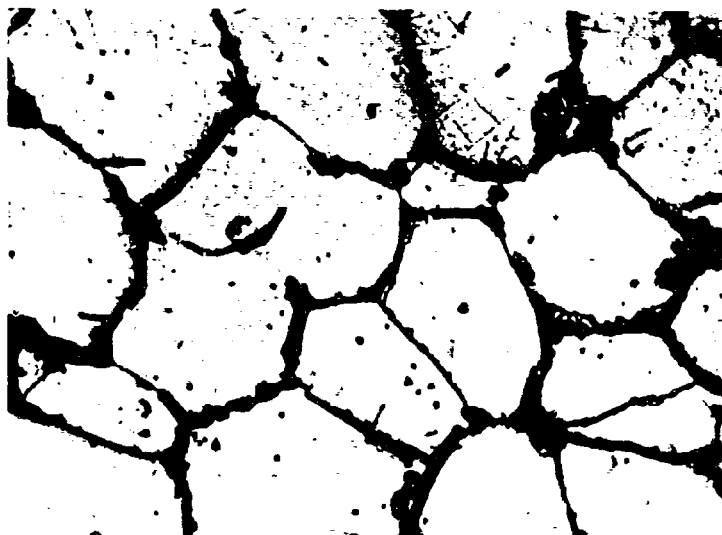


Figure 50. Ta-C (51.5 At% C), Quenched from 3480°C. X1000

TaC With Grain Boundary Graphite (TaC-Depleted Eutectic).

by differential-thermoanalytical experiments, which were carried out in 2 At% intervals within the homogeneous range of the phase, and which covered the temperature range from 800 to 3400°C.

e. Carbon-Rich Phase Equilibria

No other carbide is formed above 50 At% C, i.e. the monocarbide is in direct equilibrium with graphite over the entire solidus range. The eutectic line occurs at 3445°C as determined by melting point (Figure 19 and Table 5) as well as by DTA-investigations (Figure 51) on excess graphite containing alloys. The composition of the eutectic was bracketed to 61 ± 0.5 At% C by metallographic inspection of alloys which were quenched from above the eutectic line (Figures 52 and 53).

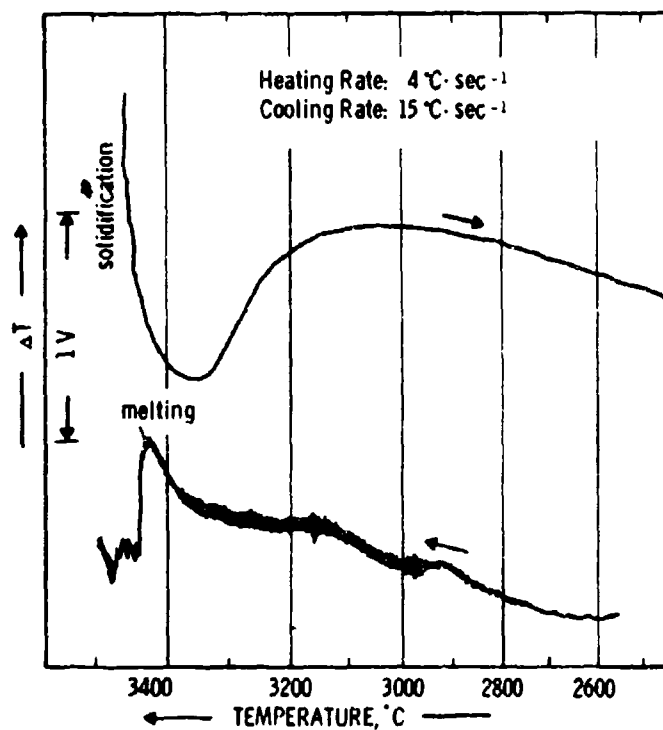


Figure 51. DTA-Thermogram of a Ta-C Alloy With 70 Atomic % Carbon, Showing Eutectic Melting (Heating) and Solidification (Cooling) at $\sim 3440^{\circ}\text{C}$.

f. Assembly of the Phase Diagram

The experimental findings have been combined in the proposed phase diagram shown in Figure 1. Although, according to the present findings, ζ is not to be considered as an equilibrium product, and hence is not to be regarded as a 'phase' in the common sense, for all practical purposes the non-equilibrium precipitation process from the substoichiometric tantalum-monocarbide has to be taken into consideration. Preferred precipitation of the non-equilibrium product has therefore

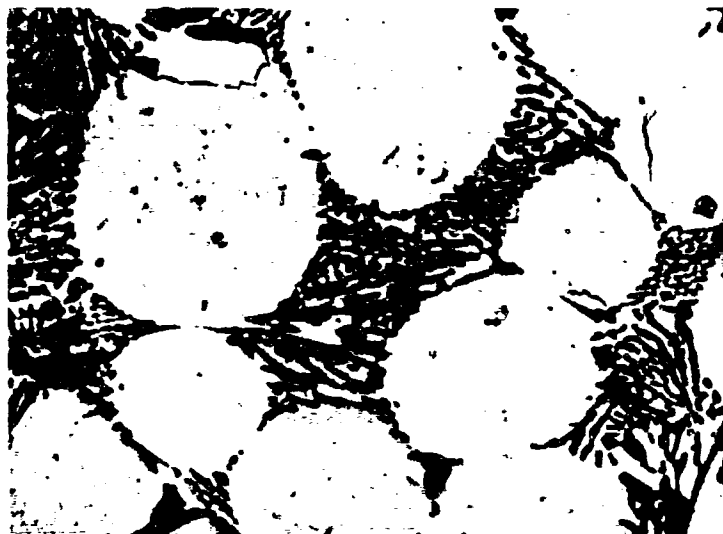


Figure 52. Ta-C (55 At% C), Quenched from 3480°C.

X1000

Primary Crystallized Monocarbide in a Eutectic
Matrix of TaC + C.

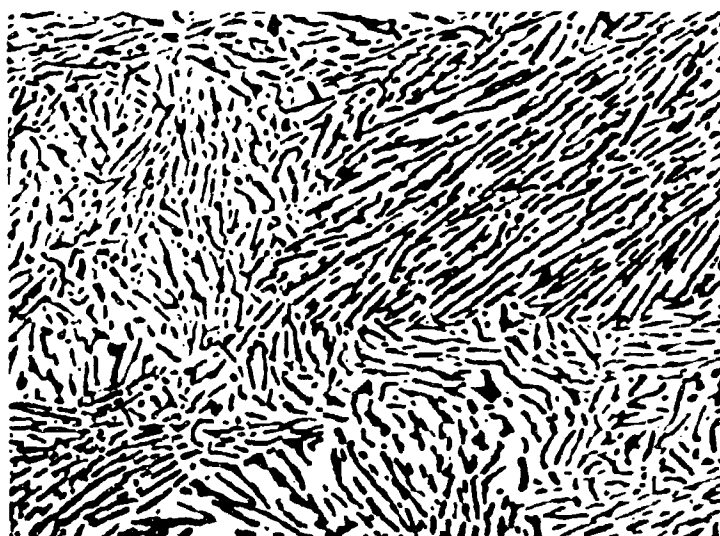


Figure 53. Ta-C (61 At% C), Quenched from 3450°C.

X1000

TaC + C Eutectic

been indicated by the shaded area shown in Figure 1. Following the experimental evidence, the α - β - Ta_2C phase reaction is assumed as a two-phase process and recorded in the phase diagram accordingly.

Above 3800°C , where the vapor pressure of pure graphite exceeds one atmosphere, the principle equilibria, i.e. the composition of the melt in equilibrium with carbon gas of 1 atmosphere pressure, are sketched into the diagram.

In order to reveal the relative accuracy of the measurements, it was decided to attach the precision of the measurements to the mean values of the measured temperatures. The uncertainty figures given, therefore do not include the calibration errors. Representative values for the standard errors in the pyrometer calibration have been presented in Section B-3, and may be used for the computation of the overall temperature uncertainties.

2. Niobium-Carbon and Vanadium-Carbon

Since Ta_2C as well as the subcarbides of the group VIa transition metals have been found to undergo phase changes at elevated temperatures, the main interest in these two metal-carbon systems concentrated the high temperature behavior of the Me_2C -phases. Relating to the Nb-C system, melting experiments in ternary alloys⁽⁴¹⁾ indicated higher melting temperatures for the monocarbide phase than reported by G.K. Storms and N. H. Krikorian⁽¹⁾. A reinvestigation of the solidus temperatures of the carbon-rich portion ($> 40 \text{ At\% C}$), was therefore included in the investigation.

The alloys for the investigation in both systems were prepared by short-duration hot-pressing of the well-mixed powders. The resulting samples were surface-ground to remove the adhering graphite skin, and were then heat-treated for 10 hrs (Nb-C alloys 1800°C, V-C alloys 1400°C) under a vacuum of better than 5×10^{-5} Torr. The DTA-runs were performed under vacuum as well as under a high purity helium atmosphere (~ 2 atm.). The melting point measurements were carried out using the previously described Pirani technique.

a. Niobium-Carbon

Five samples, with carbon contents of 25, 30, 32, 33, and 34 At% were investigated by differential thermoanalytical techniques. The temperature range covered varied from between 800 to 2700°C for alloys with carbon concentrations lower than 30 At% C, and between 800 and 3100°C for the higher carbon alloys.

The DTA-runs on the alloy with 25 atomic % carbon showed an interesting behavior: A sharply defined endotherm, identified as being due to eutectic melting was observed at approximately 2320°C on the heating cycle (Figure 54); this endotherm then was followed by a second sharp peak due to another endothermic reaction commencing at approximately 2440°C. On the cooling cycle, the arrest due to the latter reaction is superimposed on the solidification curve produced by the bivariant solidification, and was found at slightly higher temperatures than on the heating cycle. Eutectic melting was absent in the alloy with 30 At% C, and the DTA-thermograms show the α - β -Nb₂C reaction only (Figure 54). The phase reaction involves the entire homogeneity range of the phase, as evidenced

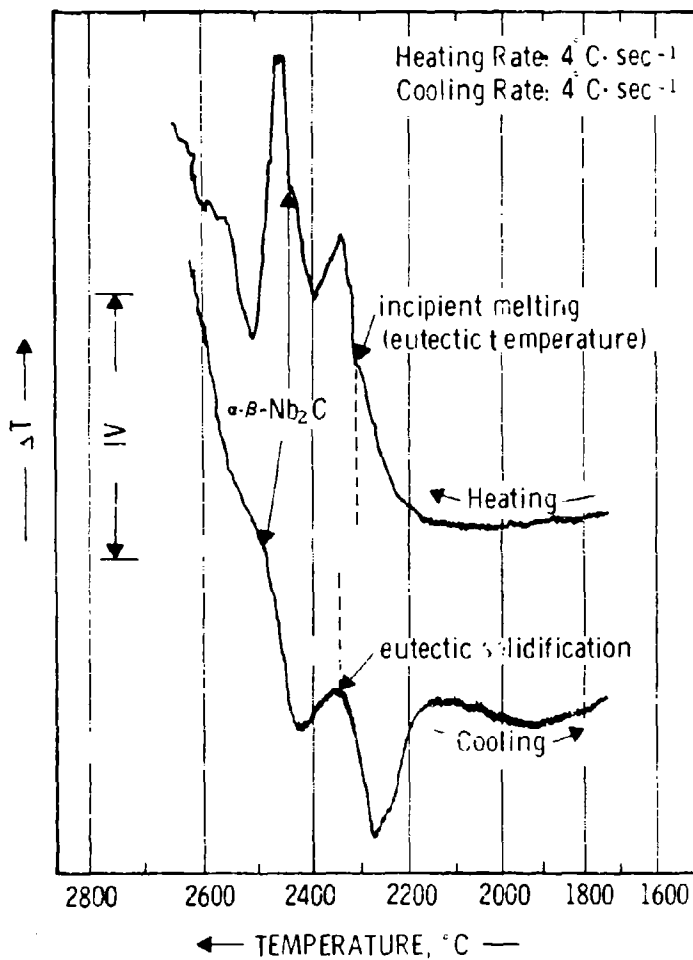


Figure 54. DTA-Thermogram of a Niobium Carbon Alloy With 25 Atomic % Carbon.

by the thermograms shown in Figure 55 and 56. A closer inspection of the curves suggests the existence of a certain concentration-temperature gap to exist between both modifications, which again would imply a two-phased process for the α - β - Nb_2C phase reaction.

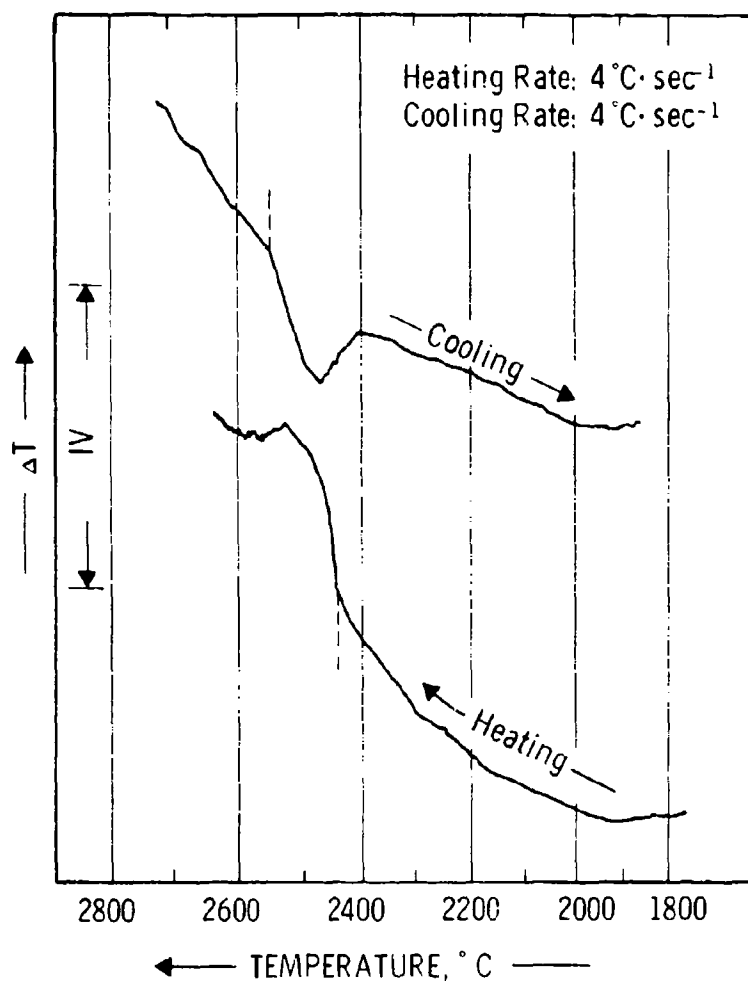


Figure 55. Differential Heating and Cooling Curve of a Niobium-Carbon Alloy with 30 Atomic % Carbon.

Although immediate proof by high temperature X-ray or neutron diffraction is not yet available, preliminary results obtained by metallographic techniques indicate a phase change comparable to that observed for Ta_2C , i.e. the transformation will be characterized by a destruction of long-range order in the carbon sublattice, without structure changes in the metal frame work.

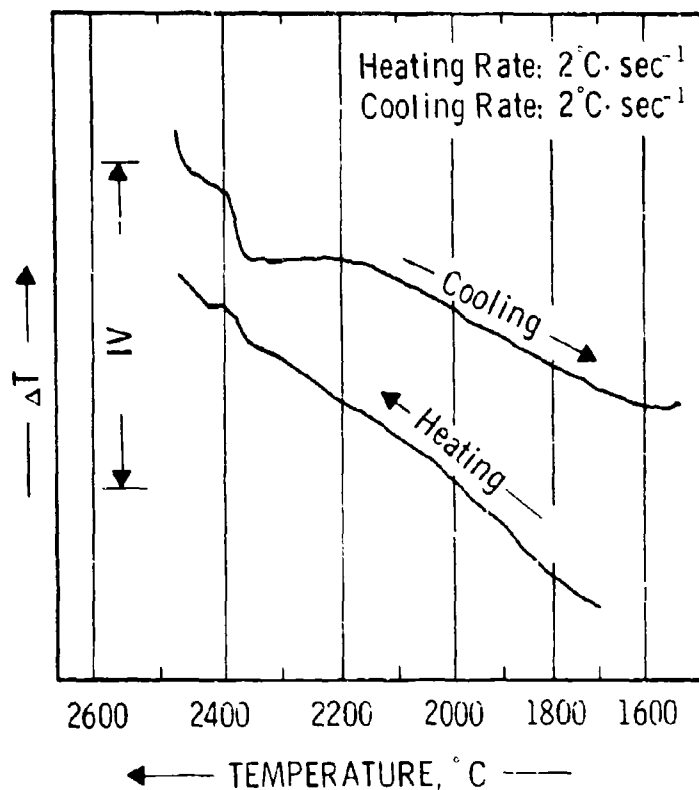


Figure 56. Differential Heating and Cooling Curve of a Niobium-Carbon Alloy with 32 Atomic % Carbon.

Melting temperatures, which are in the average 100 to 120°C higher than those obtained by Storms and Krikorian⁽¹⁾ were obtained for the monocarbide phase (Figure 2). The NbC + C reaction isotherm was found to occur at 3300°C. The eutectic composition is located close to 50 At% C.

b. Vanadium-Carbon

Two alloys with nominal carbon concentrations of 30 and 32 atomic percent were examined differential-thermoanalytically. No thermal arrests, which could be associated with an

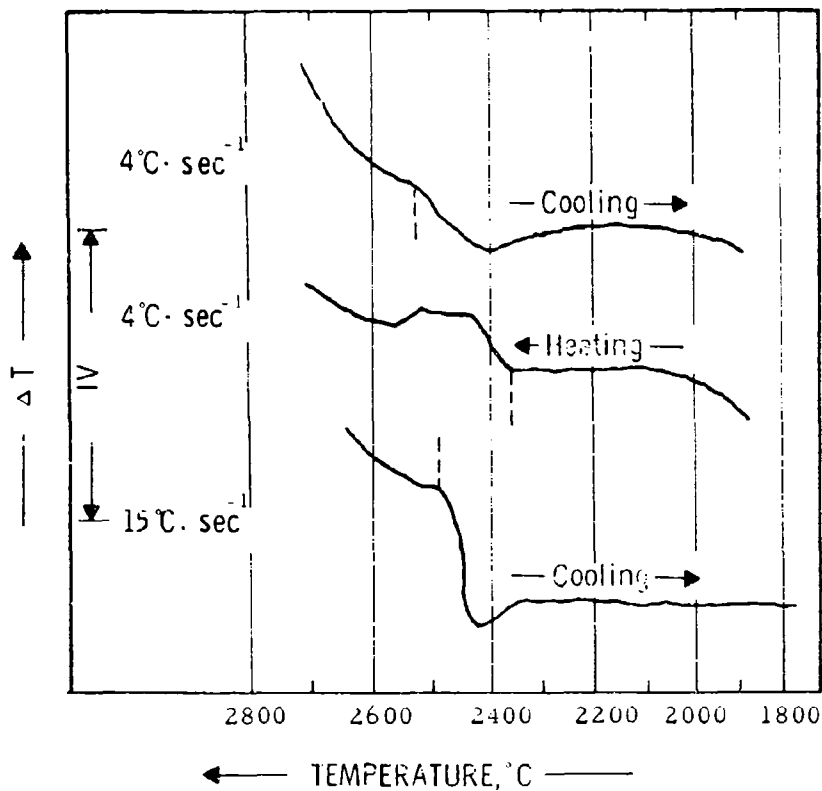


Figure 57. Differential Heating and Cooling Curves of a Niobium-Carbon Alloy with 34 Atomic % Carbon.

isothermal phase reaction were observed in these studies, which covered the temperature range from 800 to 2300°C.

Two explanations for this deviating behavior are possible: either the reaction proceeds so slow, that it could not be observed within the available rate spans of the DTA-apparatus (0.2 to $\sim 20^{\circ}\text{C}/\text{sec}$), or the carbon sublattice already is essentially disordered in the temperature range covered in the experiments. Since for each of the previously found examples (Nb_2C , Ta_2C , Mo_2C , and

W_2C) the reaction proceeds with comparable high speeds, the second assumption appears to be the more plausible. However, more detailed investigations, especially studies of the carbon distribution in long-time annealed ($< 800^\circ C$) specimens by neutron diffraction as well as determination of the thermal expansion characteristics and the low temperature heat capacities of these compounds will be necessary for a definitive answer. As a concluding remark to the exceptional behavior of V_2C , it may only be mentioned, that by substitution of vanadium by other metals, such as Mo, W, Nb, and Ta, the disordering reaction becomes observable at relatively small exchanges (~ 10 mole %). The temperature range of transformation in these solid solutions increase smoothly from $< 1000^\circ C$ at ~ 10 mole % Me_2C exchange to the transformation temperatures of the corresponding binary subcarbides. These findings strengthen the supposition of a lower ordering temperature of V_2C as compared to the other subcarbides of the refractory-transition metals.

For a comprehensive experimental and theoretical treatment of the effect of metal substitution on sublattice disorder in subcarbide phases, reference may be made to a later report.

IV. DISCUSSION

A. THE α - β - Ta_2C PHASE REACTION

Probably the most important finding of the present work concerns the conclusive establishment of the existence of high temperature phase transformations of Nb_2C and Ta_2C . As discussed previously⁽⁵⁾ it is to be expected, that this reaction type may probably be a quite common phenomenon for interstitial phases with excess vacant lattice sites. The

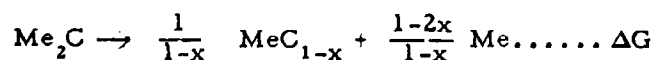
extent, to which a reaction of this type will proceed is dependent on the place-shifting energies involved, which in turn are related to the shape of the free energy curves around the stoichiometric composition. Thus, a disordering reaction of the type discussed will not generate in each instance a reaction isotherm such as the eutectoid and peritectoid found for the majority of the subcarbides of the refractory transition metals.

A difficulty with presently available theoretical approaches to the order-disorder problem seems to involve a proper analytical description of the phase conditions within the transition region. As an example, heterogeneous (two-phase) transitions between a substantially ordered and a substantially disordered phase, involving the coexistence of two phases of different stoichiometry cannot be accounted for⁽⁴³⁾.

Another important problem concerns the effect of composition upon the disordering reaction, as well as the type of order. As for the Me_2C -type compounds, which nearly exclusively show an ordered arrangement of the N carbon atoms among the 2N equivalent or quasi-equivalent (Mo_2C) interstitial lattice sites, it appears from the available data, that for the group VI metal subcarbides (Mo_2C , W_2C) the disordering reaction proceeds as a homogeneous (single-phased) process at sub-stoichiometric compositions, while stoichiometric or slightly hyper-stoichiometric compositions undergo a discontinuous phase change. On the other hand, the transition involves the whole homogeneity range of the subcarbide in the tantalum- and niobium-carbon systems; the concentration dependence of the mid-point transition temperatures in the latter systems decrease with increasing carbon content. This is in agreement with the previously established rule⁽⁵⁾.

From the available experimental knowledge, we have to interpret the observed variations in the transformation characteristics of the Me_2C -phases such, that at compositions at or close to stoichiometry, the temperature range of transformation (leading to the destruction of long-range order) will solely be governed by the energy changes involved in the disordering process. The reaction proceeds as a two-phased process, with the volume of the disordered phase (heating) gradually growing at the expense of the essentially ordered phase; this implies that both phases differ in composition in the transformation region. Since no other phases are involved in the overall reaction, the less-ordered phase ultimately will resume the overall composition of the initially ordered phase. The temperature span of transformation, i.e. the temperature range required for complete phase conversion, will on the one hand be a function of the width of the two-phase field, and on the other hand, of the temperature-concentration slopes of the phase boundaries of the coexisting phases, and thus be dependent on the difference between the eutectoid and the peritectoid temperature.

Since, as discussed earlier⁽⁵⁾, the eutectoid temperature (lower temperature stability limit for the less ordered phase) depends on the stability of the next higher metal-carbon phase, this isothermal reaction temperature will be affected significantly by the free energy of disproportionation of the subcarbide into the neighboring phases. Hence, denoting the free energy of disproportionation as the free energy change of the reaction



$$\Delta G_z = \frac{1}{1-x} \Delta G_{f, MeC_{1-x}} - \Delta G_f (Me_2C)$$

MeC_{1-x} next higher metal-carbon phase

Me metal phase

we expect⁽⁵⁾, that the eutectoid temperature decreases with increasing ΔG_z , and will be lowest for the case in which no higher carbide phase is formed (Mo-C system), it will assume its maximum possible value, when ΔG_z approaches zero (stability limit of the Me_2C -phase in the binary).

The peritectoid reaction isotherm (upper temperature stability limit of the essentially ordered phase) on the other hand is only dependent upon the free energy changes involved in converting the constituent metal lattice into a structure analogous to that of the subcarbide, and is, to a first approximation, not affected by the enthalpy of formation of the subcarbide phase.

Since, for the group V metal-carbon systems, ΔG_z , which essentially compares the thermodynamic stability of the Me_2C carbides with the mechanical mixture of monocarbide and metal, assumes rather low values (3000 to 4000 cal/mol) the three temperatures (eutectoid, peritectoid and mid-point transformation temperature) almost coincide.

Although the detailed mechanism of transformation may to a certain degree depend on the structural changes involved and therefore will vary somewhat between the individual carbides*, the overall reaction

*For example, the structural changes involved in the disordering reaction are slightly different for Mo_2C , Nb_2C , and Ta_2C and W_2C : The low temperature Mo_2C modification has an orthorhombic superstructure⁽⁴⁴⁾, while Ta_2C ⁽³⁷⁾ and W_2C ⁽³⁸⁾ have the anti-cadmium iodide structure. Nb_2C has a superstructure similar to Fe_2N ⁽³⁹⁾.

will have to be interpreted on a similar basis. Further questions which are in this connection of interest concern the variation of long range order parameter of these phases with the carbon content, and consideration of the problem, when or how far long-range order is able to prevail as the interstitial content of these phases is lowered considerably below their stoichiometric value.

Although the statistical theory of order-disorder phenomena is able to reproduce many of the experimentally observed phenomena, a more detailed treatment would be desirable. An experimental study of the subcarbides, such as the measurement of high temperature heat capacities, as well as electrical and elastic properties, should be of great value in developing a suitable model for the analytical description of these reactions. Such measurements would be especially valuable, since the redistribution of the carbon-atoms in these compounds may probably most closely be related as a one-dimensional case, for which exact solutions have been obtained by statistical means^(45, 46, 47).

B. PHASES AND PHASE EQUILIBRIA

The measured melting point of tantalum is in close agreement with other recently reported values of B. Riley ($3006 \pm 15^\circ$)⁽⁴⁸⁾, J. H. Berchtold⁽⁴⁹⁾ (3000°C), and H. K. Adenstedt, et.al.⁽⁵⁰⁾ (2997°C). Similar agreement is observed for the Ta-Ta₂C eutectic reaction temperature, where values of 2800°C (F. H. Ellinger⁽⁷⁾, 1943), 2825°C (R. V. Sara and C. E. Lowell⁽¹²⁾, 1964), and 2902°C (M. R. Nadler and C. P. Kempter⁽⁹⁾, 1960) were observed by earlier investigators. Somewhat larger scatters were obtained for the peritectic decomposition temperature of Ta₂C (3400°C ⁽⁷⁾, 3240°C ⁽¹²⁾, 3500°C ⁽⁹⁾, versus 3330°C in

our investigations), and the carbon-rich reaction isotherm, for which temperatures of 3300°C (F.H. Ellinger⁽⁷⁾), 3375°C (R. V. Sara and C. E. Lowell⁽¹²⁾), and 3310°C (K. I. Portnoi, et.al.⁽³³⁾, 1961), as reported, as compared to 3445°C, determined in this work. The temperature of 3700°C for the TaC + C eutectic reaction isotherm measured by C. P. Kempter and M. R. Nadler⁽²⁷⁾, and M. G. Bowman⁽²⁰⁾ appears to be somewhat high. Agreement within the experimental error for the congruent melting point of the monocarbide is observed between the recent value of M. G. Bowman⁽²⁰⁾ (4000 - 4200°C) and our data (3983°C at TaC_{0.89}). The majority of the previous melting point determinations on this phase either referred to compositions close to stoichiometry^(21, 22, 24) or were made under conditions, where considerable carbon losses during the experiment may have resulted in too metal-rich, and therefore lower melting compositions^(10, 23).

With a melting point of close to 4000°C, tantalum monocarbide appears as the most refractory material known to date.

REFERENCES

1. E.K. Storms and N. H. Krikorian: J.Phys.Chem. 64 (1960), 1471.
2. E.K. Storms and R.J. McNeal: J.Phys.Chem. 66 (1962), 401.
3. E. Rudy and Y.A. Chang: Plansee Proceedings 1964, pp
4. E. Rudy: 2nd Progress Report, AF 33(615)-1249 (Oct. 1964).
5. E. Rudy, St. Windisch, Y.A. Chang: AFML-TR-65-2, Part I, Vol. I (Jan. 1965).
6. E. Rudy and D. Harmon: 3rd Progress Report AF 33(615)-1249 (April 1965).
7. F. H. Ellinger: Trans. Am. Soc. Met. 31 (1943), 89.
8. M.L. Pochon, C.R. Mc Kinsey, R.A. Perkins, and W.D. Forging: "Reactive Metals, Vol. 2" (Intersc.Publ. New York, 1959).
9. M.R. Nadler and C.P. Kempter: J.Phys.Chem. 64 (1960), 1468.
10. C. F. Zalabak: NASA-TN-D-761 (1961).
11. G. Santoro and H.B. Probst: W. Mueller (Editor), "Advances in X-Ray Analysis", Vol. 7 (1963), 126 (Plenum Press, New York).
12. R.V. Sara and C.E. Lowell, WADD-TDR-60-143, Part V, (1964).
13. D.A. Vaughn, O.M. Stewart, and C.M. Schwartz: Trans. AIME, 221 (1961) 937.
14. E. Fromm and U. Roy: J. Less-Common Metals, 8 (1965), 75-77.
15. R. Lesser and G. Brauer: Z.Metallkunde 49 (1958), 622 .
16. W.G. Burgers and J.C.M. Basart: Z.anorg.allg.Chemie, 216 (1934), 209 .
17. V.I. Smirnova and B.F. Ormont: Z.Fiz.Khim., 30 (1956), 1327.
18. LB. Dubrovskaya, G.P. Shveykin, and P.V. Geld: Fiz. Metal. Metalloved., 17 (1964), 73.
19. J.G. McMullin and J.T. Norton: Trans AIME 197 (1953), 1205
20. M.G. Bowman: Paper presented at the 5th Plansee Seminar in June 1964 at Reutte, Tirol, Austria.

References (cont.)

21. E. Friederich and L. Sittig: Z. anorg.allg.Chem., 144 (1925), 174.
22. C. Agte and H. Alterthum: Z. Techn. Physik, 11 (1930), 185.
23. G.A. Geach and F.O. Jones: Met. Abstr. 24 (1957), 366.
24. L.D. Brownlee: J. Inst. Metals, 87 (1958), 58.
25. A.E. vanArkel: Physica, 4 (1924), 286.
26. K. Becker and F. Ebert: Z. Physik, 31 (1925), 268.
27. C.P. Kempter and M.R. Nadler: J. Chem. Phys, 32 (1960), 1477.
28. D.A. Robins: in "The Physical Chemistry of Metallic Solution and Intermetallic Compounds", Paper 7B (Her Majesty's Stationery Office, London, 1959).
29. A.L. Bowman: J. Phys. Chem. 65 (1961), 1596.
30. E. Rudy, El. Rudy, and F. Benesovsky: Mh. Chem. 93 (1962), 1176.
31. P.T.B. Shaffer: J. Amer. Ceram. Soc., 46 (1963), 177.
32. L.S. Levinson: J. Chem. Phys., 39 (1963), 1550.
33. K.I. Portnoi, Y.U. Levinsky, and V.I. Fadajeva: Izvest. Akad. Nauk SSSR, Otdel. Tekh. Nauk., Met. i Topliov, 2 (1961), 147.
34. W.B. Pearson: Handbook of Lattice Spacings and Structures of Metals and Alloys (Pergamon, New York, 1958).
35. H.D. Heetderks, E. Rudy, T. Eckert: AFML-TR-65-2, Part III, Volume I (May 1961); Planseeber. Pulvermet. (in print).
36. G. Santoro and H.B. Probst: NASA Lewis Laboratory, Private Communication, March 1965.
37. A.L. Bowman: Private Communication, July 1965.
38. L.N. Butonia and Z.G. Pinsker: Soviet Physics, Crystallography 5 (1960), 560.
39. Nobuzo Terao: J. Appl. Physics 3 (1964), 104.
40. R. Kieffer and F. Benesovsky: "Hartstoffe" (Wien, Springer, 1963).

References (cont.)

41. E. Rudy: AFML-TR-65-2, Part II (to be published).
42. E. Rudy and St. Windisch: AFML-TR-65-2, Part I, Vol. VI. (Sept. 1965).
43. C. Wagner: Thermodynamics of Alloys (Addison-Wesley, Reading, Mass., 1952).
44. E. Parthé and V. Sadagopan: Mh. Chem. 93, (1962), 263.
45. H. A. Kramers and G. H. Wannier: Phys. Rev. 60 (1941), 252.
46. L. Onsager: Phys. Rev. 65 (1944), 117.
47. G. H. Wannier: Rev. Mod. Phys., 17 (1945), 50.
48. B. Riley: J. Sci. Instr., 41 (1964), 504.
49. J. H. Berchtold: Acta Metallurgica, 3 (1955), 249.
50. H.K. Adenstedt, J.R. Pequino, and J.M. Raymer: Trans. ASM, 44 (1955), 249.